

## Novel 1,3-Dipropyl-8-(3-benzimidazol-2-yl-methoxy-1-methylpyrazol-5-yl)xanthines as Potent and Selective A<sub>2B</sub> Adenosine Receptor Antagonists

Pier Giovanni Baraldi,<sup>\*,†</sup> Stefania Baraldi,<sup>†</sup> Giulia Saponaro,<sup>†</sup> Delia Preti,<sup>†</sup> Romeo Romagnoli,<sup>†</sup> Laura Piccagli,<sup>§</sup> Andrea Cavalli,<sup>‡</sup> Maurizio Recanatini,<sup>‡</sup> Allan R. Moorman,<sup>||</sup> Abdel Naser Zaid,<sup>⊥</sup> Katia Varani,<sup>‡</sup> Pier Andrea Borea,<sup>‡</sup> and Mojgan Aghazadeh Tabrizi<sup>\*,†</sup>

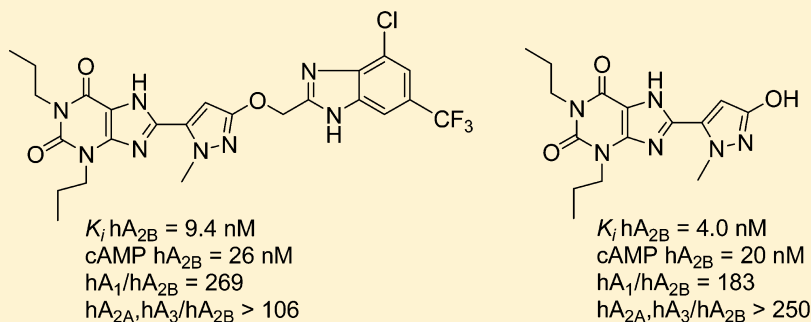
<sup>†</sup>Department of Pharmaceutical Sciences, <sup>‡</sup>Department of Clinical and Experimental Medicine, University of Ferrara, Via Fossato di Mortara 17–19, 44100 Ferrara, Italy

<sup>§</sup>Department of Biochemistry and Molecular Biology, University of Ferrara, 44100 Ferrara, Italy

<sup>||</sup>King Pharmaceuticals Inc., Research & Development, 4000 CentreGreen Way, Suite 300, Cary, North Carolina 27513, United States

<sup>⊥</sup>College of Pharmacy, An-Najah National University, Nablus, Palestine

### **S** Supporting Information



**ABSTRACT:** Molecular modeling studies, including the comparative molecular field analysis (CoMFA) method, on 52 antagonists of the A<sub>2B</sub> adenosine receptor with known biological activity were performed to identify the three-dimensional features responsible for A<sub>2B</sub> adenosine receptor antagonist activity. On the basis of these and previous results on the potent antagonist effect of 8-pyrazolyl-xanthines at human A<sub>2B</sub>AR, a new series of compounds was synthesized and evaluated in binding studies against the human A<sub>1</sub>, A<sub>2A</sub>, A<sub>3</sub>, and A<sub>2B</sub>ARs. A remarkable improvement in selectivity with respect to the previous series, maintaining the potency at human A<sub>2B</sub> receptor, was achieved, as exemplified by the 8-[3-(4-chloro-6-trifluoromethyl-1H-benzimidazol-2-yl-methoxy)-1-methyl-1H-pyrazol-5-yl]-1,3-dipropyl-3,7-dihydro-purine-2,6-dione derivative **66**:  $K_i$  hA<sub>2B</sub> = 9.4 nM, IC<sub>50</sub> hA<sub>2B</sub> = 26 nM hA<sub>1</sub>/hA<sub>2B</sub> = 269, hA<sub>2A</sub>/hA<sub>2B</sub> > 106, hA<sub>3</sub>/hA<sub>2B</sub> > 106. This study also led to the identification of a series of pyrazole-xanthine compounds with a simplified structure, exemplified by 8-(3-hydroxy-1-methyl-1H-pyrazol-5-yl)-xanthine **80** displaying very high affinity at A<sub>2B</sub>AR with good selectivity over AR subtypes ( $K_i$  = 4.0 nM, IC<sub>50</sub> hA<sub>2B</sub> = 20 nM hA<sub>1</sub>/hA<sub>2B</sub> = 183, hA<sub>2A</sub>, hA<sub>3</sub>/hA<sub>2B</sub> > 250).

### ■ INTRODUCTION

Adenosine mediates its effects through activation of a family of four G-protein coupled adenosine receptors (ARs). These receptors differ in their affinity for adenosine, in the type of G proteins that they recruit, and finally in the downstream signaling pathways that are activated in the target cells.<sup>1,2</sup>

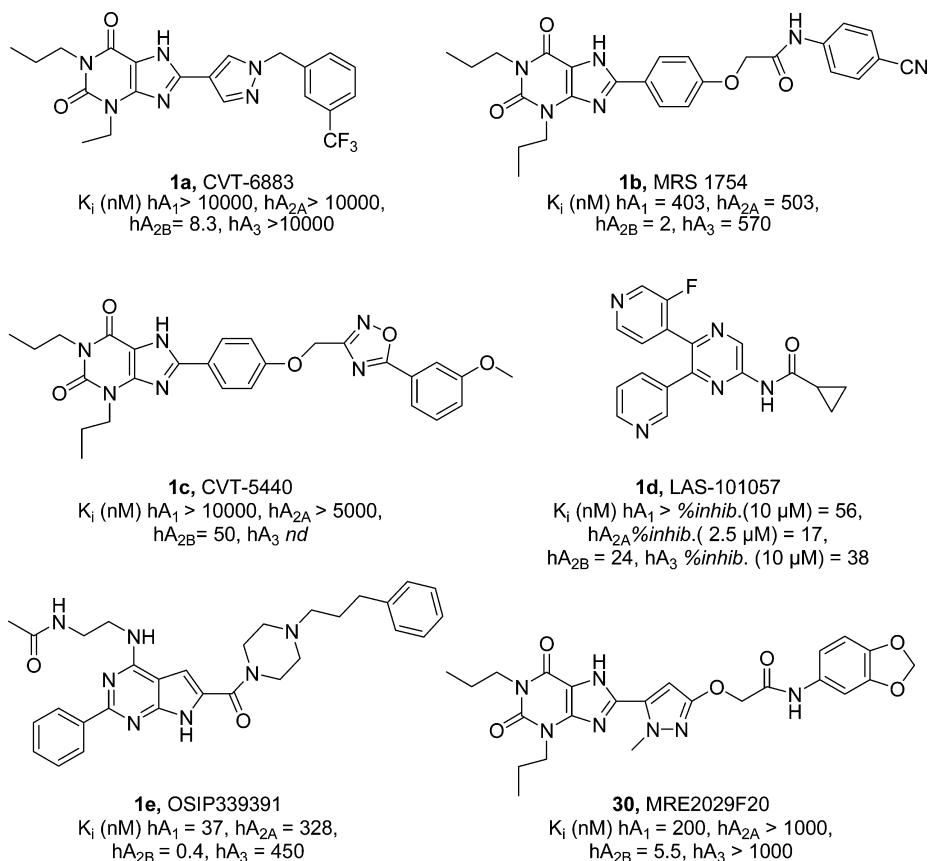
The A<sub>2B</sub>AR has long been known to couple to adenylyl cyclase activation through G<sub>s</sub> proteins. However, other intracellular signaling pathways have been demonstrated to be associated with A<sub>2B</sub>AR, including Ca<sup>2+</sup> mobilization through G<sub>q</sub> proteins and mitogen-activated protein kinase (MAPK) activation.<sup>3</sup> A<sub>2B</sub>AR-induced stimulation of phospholipase C results in mobilization of intracellular calcium in human mast cell line (HMC-1) and promotion of interleukin-8 (IL-8)

production.<sup>4</sup> Recent findings support the involvement of A<sub>2B</sub>AR subtype in adenosine-mediated coronary vasodilation.<sup>5,6</sup> Activation of A<sub>2B</sub>AR may prevent cardiac remodelling after myocardial infarction.<sup>7</sup> A protective effect from infarction has been also attributed to A<sub>2B</sub>AR in ischemic postconditioning through a pathway involving protein kinase C and phosphatidylinositol-3-kinase.<sup>8</sup>

According to mRNA analysis, revealing high levels of A<sub>2B</sub>AR message in the cecum and large intestine, it has been reported that A<sub>2B</sub>ARs in intestinal epithelial cells trigger an increase in cAMP levels that is responsible for Cl<sup>-</sup> secretion. This Cl<sup>-</sup>

Received: September 28, 2011

Published: December 12, 2011

Chart 1. Chemical Structures and Biological Data for A<sub>2B</sub>AR Antagonists

secretion pathway results in movement of isotonic fluid into the lumen, a process that naturally serves to hydrate the mucosal surface but, in extreme, produces secretory diarrhea.<sup>9–11</sup>

Adenosine constricts airways of asthmatic patients through the release of histamine and leukotrienes from sensitized mast cells.<sup>12</sup> The receptor involved seems to be the A<sub>2B</sub>AR in humans or the A<sub>3</sub>AR in rats. Recently, A<sub>2B</sub>ARs have been reported to mediate several proinflammatory effects of adenosine in inflammatory cells of the lung. In addition to mast cells, functional A<sub>2B</sub>ARs have been found in bronchial smooth muscle cells and lung fibroblasts. In these cells, adenosine increases the release of various inflammatory cytokines through stimulation of the A<sub>2B</sub> subtype, supporting the evidence that the A<sub>2B</sub>AR plays a key role in the inflammatory response associated with asthma.<sup>13–15</sup>

The first evidence for the involvement of A<sub>2B</sub>AR in asthma derived from studies concerning the selectivity of enprofylline, a methylxanthine structurally related to theophylline.<sup>16</sup> Further support for the role of A<sub>2B</sub>AR in asthma comes from studies demonstrating their presence on different type of cells important for the cytokine release in asthmatic disease such as smooth muscle cells, lung fibroblasts, endothelial cells, bronchial epithelium, and mast cells. Low expression of A<sub>2B</sub>ARs was also found in lung parenchyma of patients affected by chronic obstructive pulmonary disease (COPD).<sup>13</sup> In bronchoalveolar lavage macrophages from COPD patients, A<sub>2B</sub>ARs were downregulated compared to smokers with normal lung function. In addition, A<sub>2B</sub>AR mRNA and protein expression was selectively decreased by oxidative/nitrosative stress but not by inflammatory mediators in a human leukemic monocyte-like cell line (U937 cells) supporting the potential for modulating

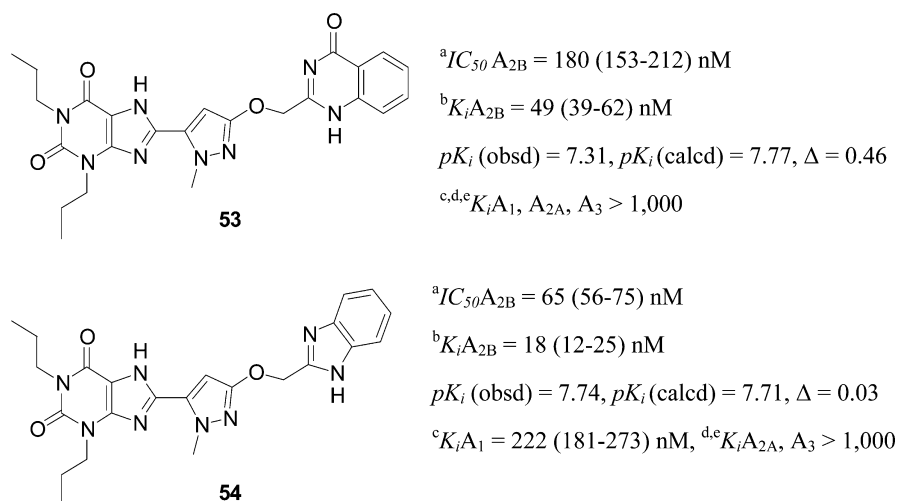
A<sub>2B</sub>AR function in alveolar macrophages as a novel treatment for COPD.<sup>17</sup>

It has been also reported that adenosine deaminase-deficient mice treated with the selective A<sub>2B</sub>AR antagonist **1a** (CVT-6883,<sup>18</sup> Chart 1) showed reduced elevations in proinflammatory cytokines and chemokines as well as mediators of fibrosis and airway destruction.

Because of the biological effects described above, selective ligands of the A<sub>2B</sub>AR could be useful as antiasthmatic and antiallergic, antidiabetic, antidiarrheal, antiatherosclerotic, and oncolytic drugs, as well as for the treatment of cardiovascular and ocular disorders.

Many selective and high affinity antagonists have been developed for adenosine A<sub>2B</sub> receptors.<sup>19–22</sup> The major representative A<sub>2B</sub>AR antagonists are shown in Chart 1. On the basis of early A<sub>2B</sub>AR selective ligands such as **1b** (MRS 1754)<sup>23</sup> ( $K_i$   $hA_{2B} = 2$  nM,  $K_i$   $hA_1 = 403$  nM,  $K_i$   $hA_{2A} = 503$ , and  $K_i$   $hA_3 = 570$  nM), several compounds have been discovered as A<sub>2B</sub>AR antagonists. Zablocki and co-workers have described the preparation and affinity of 3-phenyl-1,2,4-oxadiazoles and 5-phenyl-1,2,4-oxadiazoles as amide surrogates for **1b**. In this study, they found that the metabolic stability of MRS analogues was enhanced by replacing the anilide moiety with 1,2,4-oxadiazole nucleus. Within this series, **1c** (CVT-5440)<sup>24</sup> had the highest selectivity and an affinity of 50 nM for the A<sub>2B</sub>AR.

The 8-(4-pyrazolyl)-xanthine derivative **1a**<sup>18,25</sup> is another selective, potent, and orally available A<sub>2B</sub>AR antagonist ( $K_i$   $hA_{2B} = 22$  nM,  $K_i$   $hA_1 = 1940$  nM,  $K_i$   $hA_{2A} = 3280$  nM, and  $K_i$   $hA_3 = 1070$  nM) which had been in early clinical development for the treatment of asthma and for the treatment of cardiovascular disease. Preclinical data have also suggested its potential utility

**Chart 2. Experimental and Predicted Potencies of the Novel Antagonists at hA<sub>2B</sub>AR and Experimental Binding Affinities Measured at Other AR<sup>a</sup>**

<sup>a</sup>The predictions ( $pK_i$  calcd) were obtained by using the model A (Supporting Information Table S3). (a) Data are expressed as the geometric mean with 95% confidence limits in parentheses and derived from inhibition binding experiments and cAMP assays as described in the Experimental Section. (b) Displacement of [<sup>3</sup>H]MRE2029-F20 binding to hA<sub>2B</sub>ARs ( $n = 3-6$ ). (c) Displacement of specific [<sup>3</sup>H]DPCPX binding to hA<sub>1</sub>ARs ( $n = 3-6$ ). (d) Displacement of specific [<sup>3</sup>H]ZM241385 binding to hA<sub>2A</sub>ARs ( $n = 3-6$ ). (e) Displacement of specific [<sup>3</sup>H]MRE3008F20 binding to hA<sub>3</sub>ARs ( $n = 3-6$ ). Data are expressed as geometric means with 95% confidence limits.

in chronic obstructive pulmonary disease and pulmonary fibrosis. It is being developed by Gilead Sciences.

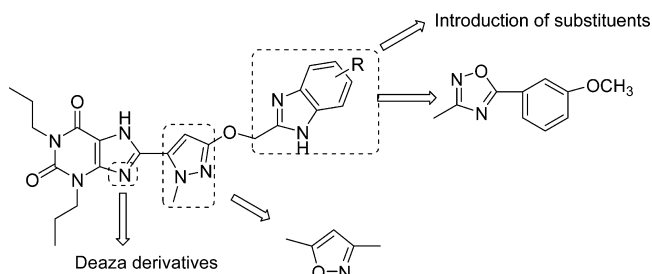
The pyrazine-based A<sub>2B</sub>AR antagonists discovered by the Almirall group include **1d** (101057),<sup>26</sup> a potent, selective, and orally efficacious A<sub>2B</sub>R antagonists that was identified as a clinical development candidate.

A novel, potent, and selective pyrrolopyrimidine A<sub>2B</sub> antagonist **1e** (OSIP339391)<sup>27</sup> was discovered by the OSI group that had a selectivity of greater than 70-fold for A<sub>2B</sub> receptors over other adenosine receptor subtypes ( $K_i$  hA<sub>2B} = 0.5 nM,  $K_i$  hA<sub>1} = 37 nM,  $K_i$  hA<sub>2A} = 328 nM, and  $K_i$  hA<sub>3} = 450 nM).</sub></sub></sub></sub>

Our group has discovered a series of 8-(5-pyrazolyl)-xanthine analogues as selective, high affinity A<sub>2B</sub>AR antagonists.<sup>28</sup> Within this series, **30** (MRE2029-F20,<sup>29</sup> Chart 1, Supporting Information Table S1) ( $K_i$  hA<sub>2B} = 5.5 nM,  $K_i$  hA<sub>1} = 200 nM,  $K_i$  hA<sub>2A}, A<sub>3} > 1000) has been radiolabeled for use in pharmacological studies.</sub></sub></sub></sub>

In the present paper, we performed a CoMFA study on the previous series of A<sub>2B</sub>AR antagonists.<sup>28</sup> In this respect, the series of antagonists is indeed uniform in terms of biological assays. The 3D QSAR model that we obtained then led to the design of two new derivatives, including a bioisosteric replacement of the anilide moiety of **30** with benzimidazole or quinazoline rings (compounds **53** and **54** respectively, Chart 2).

We then undertook the synthesis and biological evaluation of a new series of 1,3-dipropyl-xanthines that carry a *N*-methylpyrazolo or isoxazolo group at position 8. The selection of the benzimidazol-2-yl-methoxy group at the 3-position of the pyrazole/isoxazole was based on the greater potency of the benzimidazole derivative **54** over that of quinazoline **53**. In addition, the commercial availability of substituted-phenylendiamines permitted the easier optimization of the benzimidazole series. As shown in Chart 3, various structural modifications were realized using the novel A<sub>2B</sub> antagonist **54** as the template.

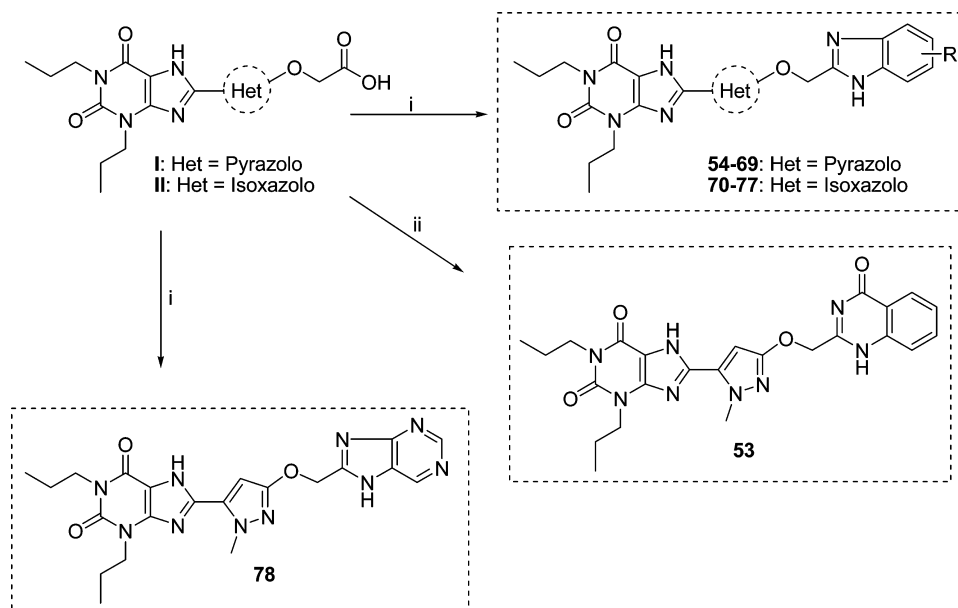
**Chart 3. Structural Modifications Considered on the 8-[3-(1*H*-Benzimidazol-2-ylmethoxy)-1-methyl-1*H*-pyrazol-5-yl]-1,3-dipropyl-3,7-dihydro-1*H*-purine-2,6-dione Template<sup>a</sup>**

<sup>a</sup>The template compound **54** is shown.

The amide bond was also replaced with the 5-phenyl-1,2,4-oxadiazole nucleus on the basis of other adenosine pharmacophores such as those reported previously by Zablocki et al.<sup>24</sup> In this context, considering the good antagonistic potencies of deaxanthines at human adenosine receptors,<sup>30,31</sup> a comparison of the affinity and selectivity profiles of 9-deaxanthines with the corresponding xanthines was afforded by the preparation of four 9-deaza direct analogues. The new compounds were tested in competitive binding assays toward four hARs expressed in CHO cells. cAMP assays were performed to determine their functionality.

## CHEMISTRY

To explore the present class of A<sub>2B</sub> antagonists, the new compounds reported in Tables 1–3 were synthesized as outlined in Schemes 1–4. The carboxylic acid derivatives **I** or **II**,<sup>28</sup> in anhydrous DMF, were condensed with phenylendiamines (as expect for compounds **53** and **78**, 2-aminobenzamide and pyrimidine-4,5-diamine were used, respectively) using 1-[3-(dimethylamino)propyl]-3-ethylcarbodiimide hydrochloride (EDC) to furnish the amides that were subsequently

Scheme 1. Preparation of Xanthine Derivatives 53–78<sup>a</sup>

<sup>a</sup>Reagents and conditions: (i) (1) appropriate diamine, EDC, DMF, rt, (2) CH<sub>3</sub>COOH, 60–70 °C; (ii) (1) 2-amino-benzamide, EDC, DMF, rt, (2) NaOH 2.5 N, 80 °C.

cyclized in the presence of acetic acid at 80–100 °C to provide the 8-heteroaryl derivatives 53–78 (Scheme 1).

The target xanthine derivatives 79 and 80 were prepared as shown in Scheme 2. 3-(Benzyloxy)-1-methyl-1*H*-pyrazole-5-carboxylic acid **V** was prepared by direct alkylation of methyl 3-hydroxy-1-methyl-1*H*-pyrazole-5-carboxylate<sup>28</sup> **III** with benzyl bromide in acetone using K<sub>2</sub>CO<sub>3</sub> as a base, followed by ester hydrolysis. Coupling of **V** with 1,3-dipropyl-5,6-diaminouracil<sup>32</sup> using EDC afforded the amide intermediate, which was cyclized in NaOH to afford compound **VI**. Debenzylation with ammonium formate and palladium-on-carbon yielded the target compound **80**. Treatment of **VI** with 2-(trimethylsilyl)-ethoxymethyl chloride (SEM-Cl) and K<sub>2</sub>CO<sub>3</sub> introduced the SEM protection group at N-7. Debenzylation yielded our key intermediate **VIII**. This compound was then alkylated with 3-chloromethyl-5-(3-methoxy-phenyl)-[1,2,4]oxadiazole<sup>33</sup> (**IX**) to yield **X**. SEM deprotection with 3 N HCl in ethanol at 80 °C afforded the target compound **79**.

The synthesis of 9-deaza-xanthines **81–84** analogues was performed as described in published procedures<sup>31,34</sup> with some modifications to reflect the change from benzaldehyde to the pyrazolo carboxaldehyde (Schemes 3 and 4).

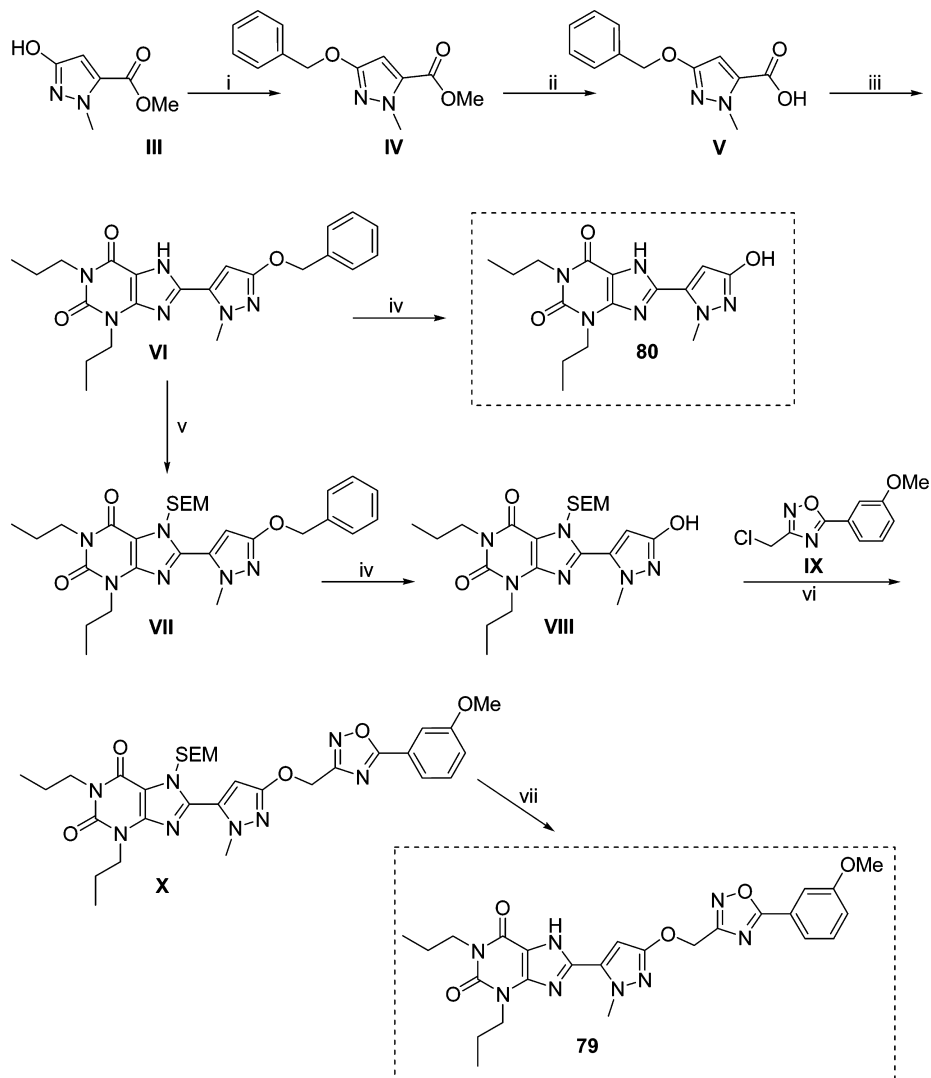
3-(Benzyloxy)-1-methyl-1*H*-pyrazole-5-carboxaldehyde **XI** was prepared by conversion of **V** into a mixed anhydride with ethyl chloroformate to yield the corresponding alcohol, which was reacted with pyridinium chlorochromate (PCC) (Scheme 3). Condensation of the 1,3-dipropyl-6-methyl-5-nitrouracil (**XII**)<sup>35</sup> with 3-benzyloxy-1-methyl-1*H*-pyrazole-5-carboxaldehyde **XI** in dry toluene and catalytic morpholine allowed us to obtain the corresponding (*E*)-6-styryl derivative **XIII** in satisfactory yields. The ring closure of **XIII** to intermediate **XIV** was performed by reductive cyclization using iron in acetic acid and ethanol under reflux. Debenzylation of **XIV** in a manner similar to that for the synthesis of **80** yielded the deaza derivative **81** (Scheme 3).

The target 9-deaza derivatives **82–84** were prepared by the same synthetic route reported for compound **81** starting from

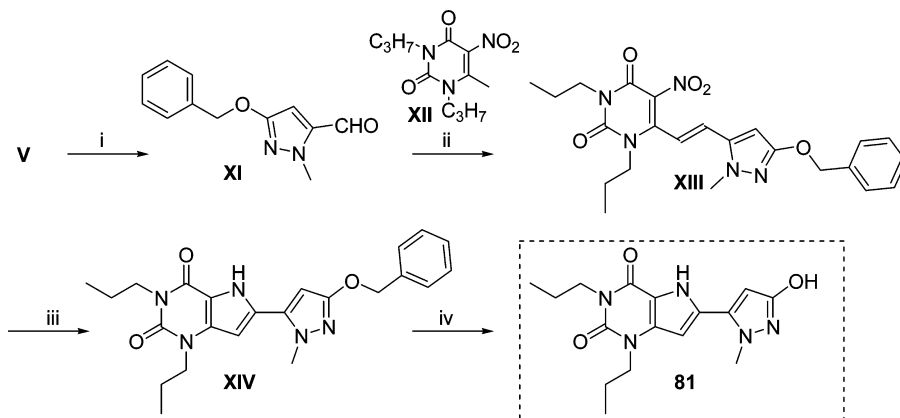
the pyrazolo carboxylic acid **XV**<sup>28</sup> to afford the intermediate pyrrolo[3,2-*d*]pyrimidin-6-yl-pyrazol-3-yloxy]-acetic acid **XIX** (Scheme 4). Target compound **82** was obtained by the same procedure used for analogues **54–69**, while direct condensation of carboxylic acid **XIX** and the suitable anilines in DMF in the presence of EDC as coupling reagent yielded **83** and **84**.

## RESULTS AND DISCUSSION

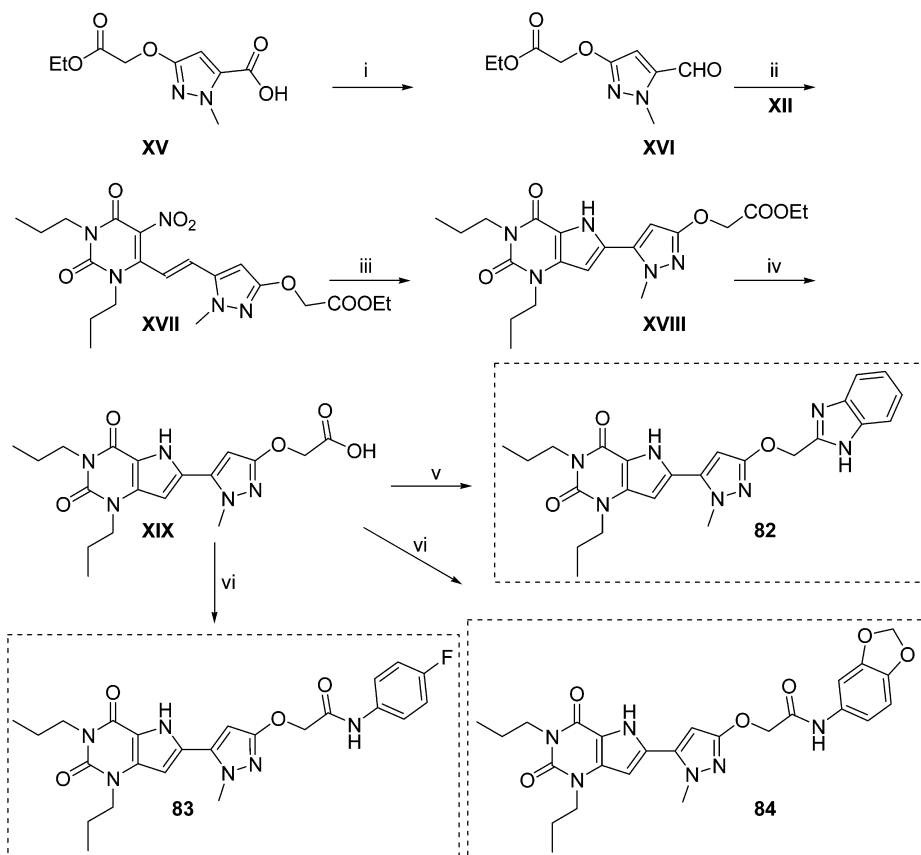
**Three-Dimensional QSAR Models.** The 3D QSAR model was developed using 52 xanthine compounds as a training set (Supporting Information Table S1). The most active compound of the series (**30**, Supporting Information Table S1, Table 3) was selected as the template for the alignment in the CoMFA analyses. A frequently used approach in pharmacophore modeling is to identify common motifs contributing to the interaction with the receptor. In the present study, the xanthine core was assumed as the common anchoring moiety, and the flexible chains linked at the 8-position were considered as biological modulators. The investigation of conformational data for the template showed the existence of several low energy structures (within an energy window of 1.0 kcal/mol). As a consequence, the selection of the candidate conformations (i.e., the putative bioactive conformations) for the eventual alignment was not trivial. To this aim, we first selected representative (i.e., the most potent) molecules (**22**, **23**, **30**, and **51**, Supporting Information Table S1) of four different subclasses of the series of compounds under investigation. Subsequently, we aligned all the low energy conformations of the four representative antagonists onto the common xanthine moiety. Considering that all ligands bind at the same site of the receptor, they should adopt a common three-dimensional geometry that is responsible for their affinity and functional activity. Thus, all the low energy conformations were clustered based on geometrical root-mean-square deviation (rmsd). On the basis of the result of the rmsd clustering procedure, two low energy conformations of compound **30** were used as templates in the following

Scheme 2. Preparation of 8-Pyrazolylxanthines 79 and 80<sup>a</sup>

<sup>a</sup>Reagents and conditions: (i) benzyl bromide,  $K_2CO_3$ , acetone, rt; (ii) KOH, dioxane, rt; (iii) (1) 5,6-diamino-1,3-dipropyl-1H-pyrimidine-2,4-dione, EDC, methanol, rt, (2) NaOH, 80 °C; (iv) Pd/C,  $HCOONH_4$ , methanol, reflux; (v) SEM-Cl,  $K_2CO_3$ , DMF, 70 °C; (vi)  $K_2CO_3$ , acetone; (vii) HCl, ethanol, 80 °C.

Scheme 3. Preparation of Deaza-xanthine 81<sup>a</sup>

<sup>a</sup>Reagents: (i) (1) ethyl chloroformate, TEA,  $NaBH_4$ , THF, -10 °C, (2) PCC,  $CH_2Cl_2$ , rt; (ii) morpholine, *pTsOH*, toluene, reflux; (iii) Fe,  $CH_3COOH$ , ethanol, reflux; (iv)  $HCOONH_4$ , Pd/C, methanol, reflux.

Scheme 4. Preparation of Deaza-xanthines 82–84<sup>a</sup>

<sup>a</sup>Reagents and conditions: (i) (1) ethyl chloroformate, TEA, NaBH<sub>4</sub>, THF, -10 °C, (2) PCC, CH<sub>2</sub>Cl<sub>2</sub>, rt; (ii) morpholine, *p*TsOH, toluene, reflux; (iii) Fe, CH<sub>3</sub>COOH, ethanol, reflux; (iv) NaOH 10%, methanol; (v) (1) 1,2-phenyldiamine, EDC, DMF, rt, (2) CH<sub>3</sub>COOH, 60 °C; (vi) aniline, EDC, DMF, reflux.

CoMFA studies. Namely, the chosen putative bioactive conformations of **30** were those placed in the two clusters with the greatest number of low energy conformations of **22**, **23**, and **51**. The statistical results of the PLS analysis were satisfactory; the best model was obtained with five latent variables (components) showing  $q^2 = 0.655$ ,  $s_{\text{cross}} = 0.290$ ,  $r^2 = 0.901$ , and  $s = 0.155$  (see Supporting Information for further details).

Steric (green and yellow) and electrostatic (blue and red) CoMFA contours are shown in Figures 1 and 2. The regions of the space around the molecule describe where the steric and the electrostatic fields have the greatest effect on binding affinity as predicted by the CoMFA model. The green and yellow zones represent regions where an increase of steric bulk increases or decreases the biological activity, respectively. The red area represents a region, where negatively charged groups favor the activity, while the blue one indicates a favorable contribution from positive groups.

The green CoMFA contour (Figure 1) located around the phenyl ring may be attributed mainly to the *N*<sup>1</sup>-methyl-pyrazole oxyacetamide derivatives (**28–40**, Supporting Information Table S1). One of the three sterically unfavorable regions (yellow in Figure 2a, left) is close to the phenyl rings of structurally different compounds: pyrazole acetamide (**7–15**, **19–21**), urea (**25–27**), and pyridine oxyacetamide (**5**) derivatives (Supporting Information Table S1). In particular, the phenyl moiety of **5** (relatively a low potency compound, orange in Figure 2a, left), protrudes completely into this

sterically negative contour map. Moreover, negative steric contours are located around the *N*<sup>1</sup>-methyl-pyrazole oxyacetamide derivatives, which bear bulky groups in the para position of the phenyl ring (**32**, **34**, **35**) (Figure 2a, right). Electrostatic negative regions are close to both the negatively charged oxygen atom of the carbonyl group and to the phenyl ring of *N*<sup>1</sup>-methyl-pyrazole oxyacetamide xanthine derivatives (**28–40**) (Figure 2b). This means that in such a region, where relatively more potent compounds containing electron-releasing functions orient their aromatic ring, an increase of negative electrostatic potential should provide more potent A<sub>2B</sub> antagonists. Concerning the positive electrostatic CoMFA contours, the main region is located around the amide hydrogen atoms of *N*<sup>1</sup>-methyl-pyrazole oxyacetamide derivatives (**28–40**) (Figure 2b).

The present CoMFA results are in a good agreement with the experimental data reported in the literature.<sup>28</sup> For instance, the good biological activity of the pyrazole oxyacetamide derivative **30** may be well explained on the basis of the present 3D QSAR model, considering that the negatively charged oxygen atom of the carbonyl group point toward the negative electrostatic regions, while the *N*-benzodioxol-phenyl structure is placed in a sterically and electrostatically favorable region (Figure 1a). In addition, the lower biological activity of **43** and **44** as compared to **28** and **29** might be due to the presence of the methyl substituent on the *N*<sup>2</sup>-position of the pyrazole structure, which forces the flexible chains of **43** (Figure 1b) and **44** far from the electrostatic and steric positive regions.

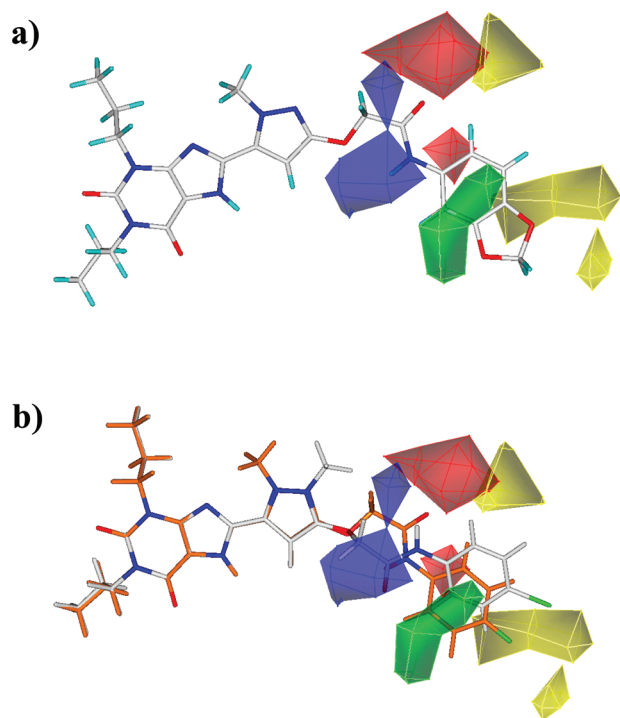


**Figure 1.** CoMFA stdev\*coeff contour plots (model A). Green contours (0.0162 level): regions where bulky groups increase activity. Yellow contours (−0.0100 level): regions where bulky groups decrease activity. Red contours (0.0150 level): regions where negative groups increase activity. Blue contours (−0.0150 level): regions where positive charge increases activity. (a) The molecule shown is the most potent compound (30). (b) The molecules shown are 28 and 43 (carbon atoms are orange).

On the basis of the CoMFA model, the new xanthine derivatives 53 and 54 (Chart 2) were designed and synthesized, and a fairly good agreement was found between the calculated and observed  $pK_i$  values (7.31 vs 7.77 and 7.74 vs 7.71, respectively; Chart 2).

**Structure–Activity Relationships.** Binding affinities of the synthesized compounds for  $A_1$ ,  $A_{2A}$ ,  $A_3$ , and  $A_{2B}$ ARs are presented in Tables 1–3. A general comparison of similarly substituted phenyl analogues between the pyrazole and isoxazole series (e.g., 56 vs 71, 59 vs 73, etc.) favors the selectivity of the pyrazole series for  $A_{2B}$ ARs versus  $A_1$ ARs.

As shown in Table 1, the parent unsubstituted phenyl analogue 54 was highly potent at the human  $A_{2B}$ AR, with a  $K_i$  value of 18 nM, although not selective for  $A_{2B}$ AR vs  $A_1$ AR ( $hA_1/hA_{2B} = 12$ ). The 5-substituted-phenyl analogues 55–60 and 62–64 showed high affinity at the  $A_{2B}$ AR, and the most potent compound was the 5-Cl derivative 56 ( $K_i A_{2B} = 5$  nM). Introducing a stronger electron-withdrawing group (Br or  $CF_3$ ) in place of the 5-Cl group, as in compounds 58 and 59, resulted in a 2–3-fold loss in binding affinity (58,  $K_i = 15.9$  nM; 59,  $K_i = 8.1$  nM). However, compound 59 showed improved selectivity for the  $A_{2B}$ AR versus the  $A_1$ AR. The 5-F derivative 55 exhibited lower affinity and selectivity in comparison to 5-Cl 56. The 5-nitro analogue 62 showed 3-fold lower affinity although comparable selectivity for the  $A_{2B}$ AR relative to the 5-Cl analogue 56.

Introduction of substituents containing a carbonyl function, such as the 5-carboxylic acid ethyl ester 63, produced good affinity and selectivity for  $A_{2B}$ AR ( $K_i = 12$  nM  $A_1/A_{2B} = 42$ ). The carboxylic acid derivative 64 exhibited less affinity at both  $A_1$  and  $A_{2B}$ AR ( $hA_{2B} K_i = 88$  nM,  $A_1/A_{2B} = 52$ ).

The 5-methoxy-phenyl analogue 57 and the 5-methyl analogue 60 had favorable binding affinities at the  $A_{2B}$ AR ( $hA_{2B} K_i = 14.2$  nM,  $hA_{2B} K_i = 10.2$  nM, respectively). They also showed greater selectivity for the  $A_{2B}$ AR versus the  $A_1$ AR, relative to 56. Shifting the methyl group from the 5- to the 4-position in analogue 65 had no significant effect on affinity or selectivity for the  $A_{2B}$ AR versus  $A_1$ AR. The 5,6-dimethyl analogue 69 was slightly less potent at  $A_{2B}$ AR ( $K_i = 22$  nM), with lower selectivity versus  $A_1$ AR, compared with 5-methyl analogue 60.

Interestingly, replacement of the phenyl ring with the naphthyl nucleus produced compound 61, which had similar

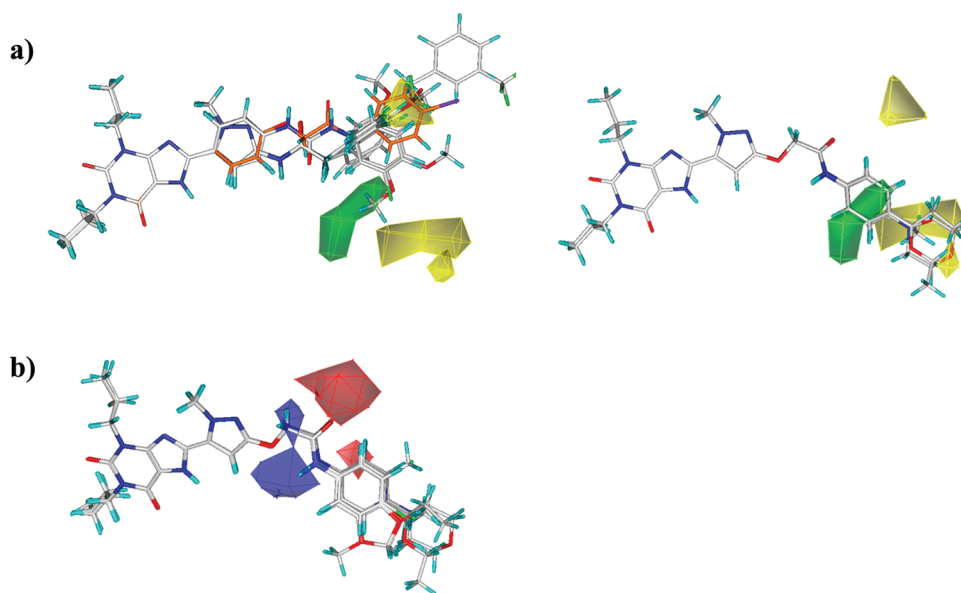
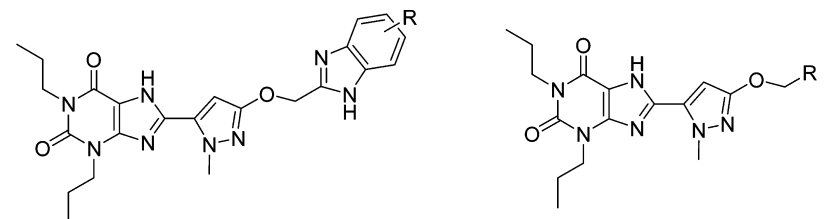


**Figure 2.** CoMFA stdev\*coeff contour plots (model A). Some aligned molecules are displayed. (a) Left: compounds 5 (carbon and hydrogen atoms are in orange), 7–15, 19–21, 25–27. Right: compounds 32, 34, and 35. (b) Compounds 28–40.

Table 1. Chemical Structures and Biological Data of Pyrazolo Xanthine Derivatives 54–69



54-69							53, 78, 79								
comp	R	hA <sub>1</sub> AR <sup>b</sup>	hA <sub>2A</sub> AR <sup>c</sup>	hA <sub>2B</sub> AR <sup>d</sup>	hA <sub>3</sub> AR <sup>e</sup>	cAMP	comp	R	hA <sub>1</sub> AR <sup>b</sup>	hA <sub>2A</sub> AR <sup>c</sup>	hA <sub>2B</sub> AR <sup>d</sup>	hA <sub>3</sub> AR <sup>e</sup>	cAMP		
		K <sub>i</sub> (nM) <sup>a</sup>							hA <sub>1</sub> /A <sub>2B</sub>	hA <sub>2B</sub> AR	K <sub>i</sub> (nM) <sup>a</sup>				
							IC <sub>50</sub> (nM) <sup>a</sup>								IC <sub>50</sub> (nM) <sup>a</sup>
54	H	222	> 1,000	18	> 1,000	12	65	64	5-COOH	4558	> 1,000	88	> 1,000	52	220
		(181-273)		(12-25)			(56-75)			(3953-5255)	(75-104)			(183-266)	
55	5-F	645	> 1,000	30	> 1,000	22	95	65	4-CH <sub>3</sub>	685	> 1,000	14.1	> 1,000	49	60
		(560-744)		(24-39)			(86-105)			(593-792)	(9.3-21.3)			(51-70)	
56	5-Cl	150	> 1,000	5.0	> 1,000	30	15	66	4-Cl 6-CF <sub>3</sub>	2530	> 1,000	9.4	> 1,000	269	26
		(107-210)		(3.6-7.0)			(11-21)			(2267-2824)	(8.8-9.9)			(17-38)	
57	5-OCH <sub>3</sub>	752	> 1,000	14.2	> 1,000	53	54	67	4,6 CF <sub>3</sub>	4462	> 1,000	25	> 1,000	178	70
		(665-851)		(7.8-25.7)			(39-76)			(4020-4952)	(20-31)			(59-84)	
58	5-Br	280	> 1,000	15.9	> 1,000	18	62	68	5-Cl 6-F	210	> 1,000	19	> 1,000	11	32
		(245-319)		(14.5-17.3)			(54-72)			(192-229)	(15-24)			(24-42)	
59	5-CF <sub>3</sub>	576	> 1,000	8.1	> 1,000	71	38	69	5,6 CH <sub>3</sub>	734	> 1,000	22	> 1,000	33	53
		(532-625)		(4.6-14.1)			(31-52)			(613-879)	(16-31)			(37-75)	
60	5-CH <sub>3</sub>	736	> 1,000	10.2	> 1,000	72	45	53		> 1,000	> 1,000	49	> 1,000	>20	180
		(666-814)		(5.0-20.5)			(37-55)				(39-62)			(153-212)	
61	5,6-C <sub>2</sub> H <sub>4</sub>	> 1000	> 1,000	20	> 1,000	> 50	80	78		> 1,000	> 1,000	> 1000	> 1,000	-	> 1,000
				(13-30)			(63-100)								
62	5-NO <sub>2</sub>	155	> 1,000	14.8	> 1,000	10	62	79		> 1,000	> 1,000	61	> 1,000	>16	219
		(133-180)		(10.2-21.5)			(54-72)				(49-77)			(186-259)	
63	5-COOC <sub>2</sub> H <sub>5</sub>	503	> 1,000	12	> 1,000	42	35								
		(476-532)		(11.4-12.5)			(29-42)								

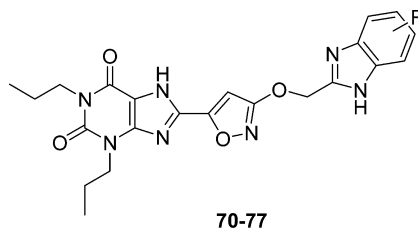
<sup>a</sup>The data are expressed as the geometric mean with 95% confidence limits in parentheses and derived from inhibition binding experiments and cAMP assays as described in the Experimental Section. <sup>b</sup>Displacement of specific [<sup>3</sup>H]DPCPX binding to hA<sub>1</sub>ARs (*n* = 3–6). <sup>c</sup>Displacement of specific [<sup>3</sup>H]ZM241385 binding to hA<sub>2A</sub>ARs (*n* = 3–6). <sup>d</sup>Displacement of specific [<sup>3</sup>H]MRE2029-F20 binding at hA<sub>2B</sub>ARs (*n* = 3–6). <sup>e</sup>Displacement of specific [<sup>3</sup>H]MRE3008-F20 binding to hA<sub>3</sub>ARs (*n* = 3–6). Data are expressed as geometric means with 95% confidence limits.

binding affinity ( $K_i = 20$  nM) as the unsubstituted phenyl analogue **54**, while it showed nearly 10-fold more selectivity for the A<sub>2B</sub>AR versus A<sub>1</sub>AR, suggesting the presence of an increased binding domain in the A<sub>2B</sub>AR versus the A<sub>1</sub>AR.

The 4,6-disubstituted analogue **66** showed high affinity and selectivity at A<sub>2B</sub>AR. In fact, compound **66** (4-Cl, 6-CF<sub>3</sub>) is the most selective analogue among the two classes of synthesized compounds ( $K_i = 9.4$  nM A<sub>1</sub>/A<sub>2B</sub> = 269). Introducing a stronger electron-withdrawing group (CF<sub>3</sub>) in place of the 4-Cl group, such as in compound **67** (4,6-CF<sub>3</sub>), resulted in a 3-fold loss in binding affinity ( $K_i = 25$  nM). The 5-Cl, 6-F analogue **68** displayed similar affinity as the 5,6-dimethyl-substituted analogue **69**, even though the 5,6-dimethyl substitution produced a 3-fold increase in selectivity versus the A<sub>1</sub>AR.

In general, the benzimidazole-isoxazole series was less selective for the A<sub>2B</sub>AR versus the A<sub>1</sub>AR when compared to the benzimidazole-pyrazole class of compounds. These data are in contrast with the pyrazole-oxacetamide derivatives synthesized in our previous work<sup>28</sup> that were more selective when compared to the pyrazole parent compounds. A similar trend was observed when comparing the isoxazole analogue **70** to the pyrazole analogue **54**. The 5-halogen analogues **71–73** displayed similar affinities at the A<sub>2B</sub>AR compared to that of the 5-halogen-substituted pyrazole analogues (**55**, **56**, **58**) but were slightly less selective versus the A<sub>1</sub>AR. A noticeable exception was the 5-bromo analogue **72** that was 4-fold more active at A<sub>2B</sub>AR in comparison to analogue **58**. Further substitution of the 5-position of the phenyl ring by a methoxy

Table 2. Chemical Structures and Biological Data of 8-Heterocyclyl Xanthine Derivatives 70–77



compd	R	$K_i$ (nM) <sup>a</sup>				$hA_1/A_{2B}$	cAMP $hA_{2B}$ AR IC <sub>50</sub> (nM) <sup>a</sup>
		$hA_1$ AR <sup>b</sup>	$hA_{2A}$ AR <sup>c</sup>	$hA_{2B}$ AR <sup>d</sup>	$hA_3$ AR <sup>e</sup>		
70	H	277 (227–338)	>1000	23 (17–30)	>1000	12	74 (65–84)
71	5-Cl	66 (57–76)	>1000	3.5 (2.9–4.2)	>1000	19	6.4 (4.9–8.3)
72	5-Br	89 (77–104)	>1000	4.1 (2.9–5.7)	>1000	22	11 (7–17)
73	5-CF <sub>3</sub>	175 (134–229)	>1000	10.0 (7.5–13.1)	>1000	18	51 (38–68)
74	5-OCH <sub>3</sub>	304 (257–361)	>1000	35 (27–47)	>1000	9	114 (86–151)
75	5-Cl, 6-F	65 (55–78)	>1000	5.5 (4.8–6.3)	>1000	12	8.0 (7.2–8.9)
76	4-Cl, 6-CF <sub>3</sub>	>1,000	>1000	22 (16–31)	>1000	>50	64 (50–81)
77	4,6 CF <sub>3</sub>	>1,000	>1000	76 (65–87)	>1000	>13	197 (136–287)

<sup>a</sup>The data are expressed as the geometric mean with 95% confidence limits in parentheses and derived from inhibition binding experiments and cAMP assays as described in the Experimental Section. <sup>b</sup>Displacement of specific [<sup>3</sup>H]DPCPX binding to  $hA_1$ ARs ( $n = 3–6$ ). <sup>c</sup>Displacement of specific [<sup>3</sup>H]ZM241385 binding to  $hA_{2A}$ ARs ( $n = 3–6$ ). <sup>d</sup>Displacement of specific [<sup>3</sup>H]MRE2029-F20 binding at  $hA_{2B}$ ARs ( $n = 3–6$ ). <sup>e</sup>Displacement of specific [<sup>3</sup>H]MRE3008-F20 binding to  $hA_3$ ARs ( $n = 3–6$ ). Data are expressed as geometric means with 95% confidence limits.

group produced compound **74** that was both less potent ( $hA_{2B}$   $K_i = 35$  nM) than **57** ( $hA_{2B}$   $K_i = 14.2$  nM) and less selective versus the  $A_1$ AR.

The introduction of a fluorine in the *ortho*-position of the 5-chloro analogue **71** produced nonsignificant effects on affinity and selectivity at  $A_{2B}$ AR, as shown by analogue **75**. In the isoxazole series, as with the pyrazole analogues, the most selective compound was the 4-Cl,6-CF<sub>3</sub>-disubstituted phenyl analogue **76** ( $hA_{2B}$   $K_i = 22$  nM,  $hA_1/hA_{2B} > 50$ ). Introduction of a trifluoromethyl group at the 4- and 6-positions produced a decrease of affinity and selectivity, such as in compound **77** in comparison with analogue **67**.

The enlargement of the benzimidazole nucleus, suggested from modeling studies, did not improve affinity at the  $A_{2B}$ AR, as demonstrated by 4-oxo-3,4-dihydro-quinazoline **53** (Table 1) but did increase the selectivity 3-fold versus  $A_1$ AR. Replacement of the phenyl ring with a pyrimidine, such as in compound **78**, afforded a complete loss of affinity at the  $A_{2B}$ AR. The benzimidazole nucleus was also replaced by 5-*m*-methoxyphenyl-1,2,4-oxadiazole to afford analogue **79** ( $K_i = 61$  nM). This analogue displayed 5-fold lower affinity compared to the 5-(methoxy)benzimidazole analogue **57** (Tables 1 and 2; Figure 3A).

The 8-(3-hydroxy-1-methyl-1H-pyrazol-5-yl)-xanthine **80** was synthesized as a simplified chemical structure of the pyrazole-xanthine series. This compound displayed very high affinity at  $A_{2B}$ AR with good selectivity over  $A_1$ AR. (Table 3,  $K_i = 4.0$  nM,  $hA_1/hA_{2B} = 183$ ; Figure 3A).

The 9-deaza-xanthines **81–84**, differing by the absence of a nitrogen atom at the 9-position of the heterocyclic xanthine system, were synthesized based on their noted antagonistic activity at the  $A_{2B}$  receptor.<sup>30,34</sup> The AR binding affinities of the deaza analogues, in comparison with the corresponding xanthines, are reported in Table 3. The analogues **83** and **85** were prepared comparing to those recently published 8-pyrazolyl-oxyacetamide derivatives<sup>24,28</sup> **28** and **30**.

In general, the new deaza analogues showed less selectivity over  $A_1$ AR, even though they displayed high affinity at  $A_{2B}$ AR.

The deaza analogue **81**, compared to **80**, displayed 2-fold less affinity at  $A_{2B}$ AR and 10-fold less selectivity versus  $A_1$ AR. The deaza analogue **82** showed an affinity comparable to the xanthine derivative **54**, although it was 4-fold less selective versus  $A_1$ AR. The deaza oxyacetamides **83** and **84** showed less affinity and selectivity at  $A_{2B}$ AR relative to the corresponding xanthine analogues **28** and **30**.

The compounds were also tested in cAMP assays, evaluating their capability to inhibit NECA-stimulated cAMP production (Tables 1–3). The majority of these ligands showed IC<sub>50</sub> values in the nanomolar range, suggesting good potency in cAMP assays. Figure 3B shows concentration–response curves of some of the most interesting compounds.

All ligands tested in functional assays *in vitro* showed very interesting antagonist activities to  $hA_{2B}$ AR, in good agreement with their affinities measured in the binding assays. (Figure 3C)

## CONCLUSION

In this paper, we constructed a 3D QSAR model for xanthine antagonists at the  $A_{2B}$ AR. Such a model was then validated by synthesizing two new xanthine compounds which displayed good agreement between the observed and calculated  $pK_i$  values.

To further explore the potential of the 8-pyrazolyl-xanthine chemotype, we synthesized a series of novel potent  $A_{2B}$ AR antagonists by varying the pyrazole moiety. Compound **66** (8-[3-(4-chloro-6-trifluoromethyl-1H-benzimidazol-2-yl-methoxy)-1-methyl-1H-pyrazol-5-yl]-1,3-dipropyl-xanthine) displayed high affinity ( $K_i = 9.4$  nM) and selectivity for the  $A_{2B}$ AR relative to the  $A_1$ ,  $A_{2A}$ , and  $A_3$ ARs. In addition, this study led to the identification of compound **80** (8-(3-hydroxy-1-methyl-1H-pyrazol-5-yl)-1,3-dipropylxanthine;  $K_i = 4$  nM). To the best of our knowledge, this compound has the highest reported affinity and selectivity described, thus far. These target compounds show high potency in inhibiting the accumulation of NECA-induced cAMP in HEK- $A_{2B}$ AR, with IC<sub>50</sub> values of 26 and 20 nM, respectively. These selective  $A_{2B}$ AR antagonists can be useful in understanding the physiological role of the  $A_{2B}$ AR

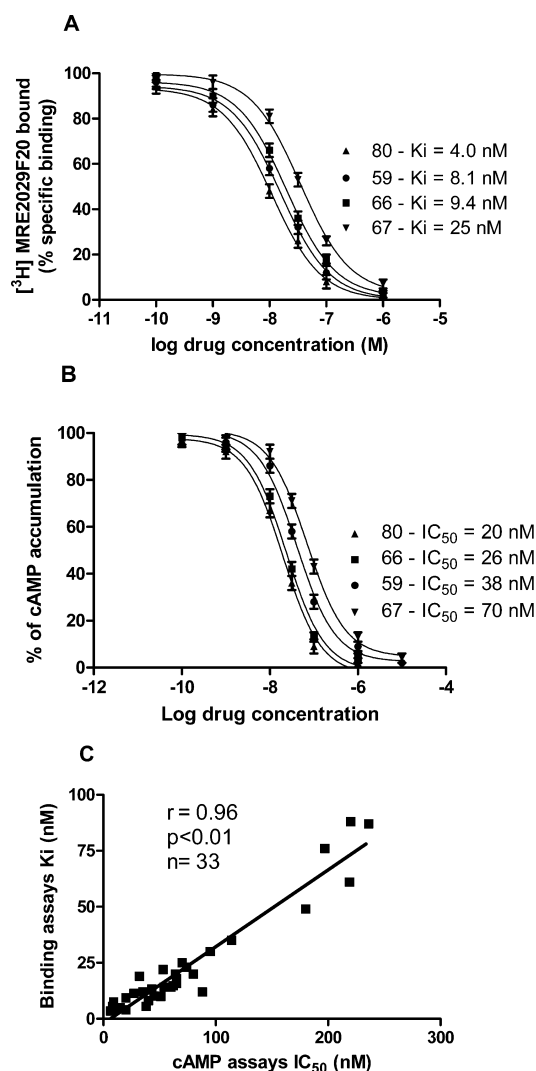


**Figure 3.** Competition binding and functional assays. (A) Affinity ( $K_i$ ) of selected novel adenosine compounds. (B) Potency ( $\text{IC}_{50}$ ) of selected novel adenosine compounds. (C) Correlation between binding and functional parameters of the novel adenosine compounds.

and may serve as leads toward the discovery of therapeutically useful agents for the treatment of asthma.

## EXPERIMENTAL SECTION

Reagent grade solvents were dried according to standard techniques. Sodium sulfate was used as a drying agent for water containing organic phases. All reported yields are of isolated products and are not optimized. Reactions were routinely monitored by thin-layer chromatography (TLC) on silica gel (F245 Merck plates). Chromatographic spots were visualized by UV light. Purification of crude compounds and separation of reaction mixtures were carried out by column chromatography on silica gel 60 (230–400 mesh from Merck). Melting points (uncorrected) were determined in a 240 Buchi-Tottoli melting point apparatus. Chemical shifts ( $\delta$ ) are reported in parts per million (ppm) relative to the solvent central peak.  $^1\text{H}$  NMR spectra were recorded at 200 MHz on a Bruker AC 200 spectrometer. Electron spray ionization mass spectrometry (ESI/MS) was performed with an Agilent 1100 series LC/MSD model in positive scan mode. The molecular weights from the MS spectra were in full agreement with the proposed chemical structures of target compounds. Elemental analyses were performed by the microanalytical laboratory of Dipartimento di Chimica, University of Ferrara, and were within  $\pm 0.4\%$  of the theoretical values for C, H, and N. All final

compounds revealed a purity of not less than 95%. The mass spectra were obtained on a ESI Micromass ZMD 2000 mass spectrometer.

**8-[1-Methyl-3-[(4-oxo-1,4-dihydroquinazolin-2-yl)methoxy]-1H-pyrazol-5-yl]-1,3-dipropyl-3,7-dihydro-1H-purine-2,6-dione (53).** To a solution of I (100 mg, 0.25 mmol) and EDC (60 mg, 0.30 mmol) in DMF (5 mL) was added 2-aminobenzamide (35 mg, 0.25 mmol). The reaction mixture was stirred at room temperature for 2 h. The solvent was evaporated in vacuo and the residue poured into water. The amide intermediate was filtered and reacted with NaOH (2.5 N, 4 mL) at 80 °C for 2 h. After cooling to 0 °C, the reaction was acidified to pH 2–3, the resultant solid was filtered and washed with water. The residue was purified by column chromatography (ethyl acetate/methanol 9:1). Yield, 60%; mp >300 °C.

$^1\text{H}$  NMR (200 MHz, DMSO- $d_6$ ):  $\delta$  0.82–0.91 (m, 6H), 1.56 (q,  $J = 7.4$  Hz, 2H), 1.72 (q,  $J = 7.0$  Hz, 2H), 3.85 (t,  $J = 7.2$  Hz, 2H), 4.03 (t,  $J = 6.6$  Hz, 2H), 4.07 (s, 3H), 5.08 (s, 2H), 6.50 (s, 1H), 7.52–8.17.82 (m, 3H), 8.10–8.14 (m, 1H), 12.55 (bs, 1H), 13.88 (bs, 1H). MS  $m/z$  491 (M  $\text{H}^+$ ). Anal. ( $\text{C}_{24}\text{H}_{26}\text{N}_8\text{O}_4$ ) C, H, N.

**8-[3-(1H-Benzimidazol-2-ylmethoxy)-1-methyl-1H-pyrazol-5-yl]-1,3-dipropyl-3,7-dihydro-purine-2,6-dione 54–69 and 8-[3-(1H-Benzimidazol-2-ylmethoxy)-isoxazol-5-yl]-1,3-dipropyl-3,7-dihydro-purine-2,6-dione (70–77).** *General Procedure.* (Except Compound 64 That Was Prepared from 63). To a mixture of the carboxylic acid (I or II, see Scheme 1) (0.25 mmol), EDC (0.25 mmol), and anhydrous DMF (5 mL) was added the appropriate phenylenediamine (0.25 mmol), and the mixture was stirred at room temperature for 20 h under argon atmosphere. The resulting solution was evaporated under reduced pressure, and the residue was dissolved in acetic acid (5 mL) and heated under stirring at 60–70 °C for 1 h. The resulting solution was cooled to room temperature and poured into water. The precipitate was collected by filtration and washed with water. The resulting crude was purified by flash column chromatography on silica gel or crystallized when necessary.

**8-[3-(1H-Benzimidazol-2-ylmethoxy)-1-methyl-1H-pyrazol-5-yl]-1,3-dipropyl-3,7-dihydro-purine-2,6-dione (54).** Purification by crystallization from dioxane. Yield 96%; mp 290 °C.  $^1\text{H}$  NMR (200 MHz, DMSO- $d_6$ ):  $\delta$  0.83–0.90 (m, 6H), 1.53 (q,  $J = 7.2$  Hz, 2H), 1.70 (q,  $J = 7.2$  Hz, 2H), 3.84 (t,  $J = 7.8$  Hz, 2H), 3.98 (t,  $J = 7.0$  Hz, 2H), 4.08 (s, 3H), 5.35 (s, 2H), 6.53 (s, 1H), 7.16–7.75 (m, 4H), 12.63 (bs, 1H), 14.00 (bs, 1H). MS  $m/z$  443 (M  $\text{H}^+$ ). Anal. ( $\text{C}_{23}\text{H}_{26}\text{N}_8\text{O}_3$ ) C, H, N.

**8-[3-(5-Fluoro-1H-benzimidazol-2-ylmethoxy)-1-methyl-1H-pyrazol-5-yl]-1,3-dipropyl-3,7-dihydro-purine-2,6-dione (55).** Purification by using column chromatography (ethyl acetate). Yield 48%; mp 280 °C.

$^1\text{H}$  NMR (200 MHz, DMSO- $d_6$ ):  $\delta$  0.83–0.92 (m, 6H), 1.57 (q,  $J = 7.0$  Hz, 2H), 1.72 (q,  $J = 7.2$  Hz, 2H), 3.86 (t, 2H), 4.01 (t, 2H), 4.15 (s, 3H), 5.36 (s, 2H), 6.54 (s, 1H), 7.00–7.68 (m, 3H), 12.77 (bs, 1H), 13.97 (bs, 1H). MS  $m/z$  481 (M  $\text{H}^+$ ). Anal. ( $\text{C}_{23}\text{H}_{25}\text{FN}_8\text{O}_3$ ) C, H, N.

**8-[3-[(5-Chloro-1H-benzimidazol-2-yl)methoxy]-1-methyl-1H-pyrazol-5-yl]-1,3-dipropyl-3,7-dihydro-1H-purine-2,6-dione (56).** Purification by crystallization from dioxane/Et $_2$ O. Yield 52%; mp 285–286 °C.

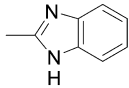
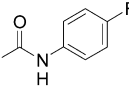
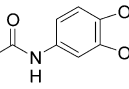
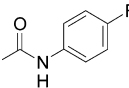
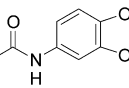
$^1\text{H}$  NMR (200 MHz, DMSO- $d_6$ ):  $\delta$  0.83–0.92 (m, 6H), 1.57 (q,  $J = 7.2$  Hz, 2H), 1.73 (q,  $J = 7.6$  Hz, 2H), 3.86 (t,  $J = 7.2$  Hz, 2H), 4.01 (t,  $J = 7.2$  Hz, 2H), 4.12 (s, 3H), 5.38 (s, 2H), 6.53 (s, 1H), 7.21–7.67 (m, 3H), 12.92 (bs, 1H), 13.97 (bs, 1H). MS  $m/z$  497 (M  $\text{H}^+$ ). Anal. ( $\text{C}_{23}\text{H}_{25}\text{ClN}_8\text{O}_3$ ) C, H, N.

**8-[3-(5-Methoxy-1H-benzimidazol-2-ylmethoxy)-1-methyl-1H-pyrazol-5-yl]-1,3-dipropyl-3,7-dihydro-purine-2,6-dione (57).** Purification by crystallization from dioxane/water. Yield 55%; mp 271 °C.

$^1\text{H}$  NMR (200 MHz, DMSO- $d_6$ ):  $\delta$  0.83–0.92 (m, 6H), 1.57 (q,  $J = 7.2$  Hz, 2H), 1.73 (q,  $J = 7.2$  Hz, 2H), 3.77 (s, 3H), 3.86 (t,  $J = 7.2$  Hz, 2H), 4.00 (t,  $J = 7.0$  Hz, 2H), 4.10 (s, 3H), 5.31 (s, 2H), 6.53 (s, 1H), 6.79–7.58 (m, 3H), 12.48 (bs, 1H), 13.97 (bs, 1H). MS  $m/z$  493 (M  $\text{H}^+$ ). Anal. ( $\text{C}_{24}\text{H}_{28}\text{N}_8\text{O}_4$ ) C, H, N.

**8-[3-(5-Bromo-1H-benzimidazol-2-ylmethoxy)-1-methyl-1H-pyrazol-5-yl]-1,3-dipropyl-3,7-dihydro-purine-2,6-dione**

Table 3. Chemical Structures and Binding Affinities ( $K_i$ ) at AR of Various Sets of Xanthines and Corresponding 9-Deaza Derivatives<sup>f</sup>

comp	X	R	$K_i$ (nM) <sup>a</sup>				cAMP	
			hA <sub>1</sub> AR <sup>b</sup>	hA <sub>2A</sub> AR <sup>c</sup>	hA <sub>2B</sub> AR <sup>d</sup>	hA <sub>3</sub> AR <sup>e</sup>	hA <sub>2B</sub> AR	IC <sub>50</sub> (nM) <sup>a</sup>
			733		4.0			20
80	N	-	(661-812)	> 1,000	(2.5-6.4)	> 1,000	183	(14-29)
81	C	-	(123-159)	960	(7.1-8.0)	> 1,000	19	(7.3-11)
82	C		(27-42)	> 1,000	(11-11.9)	> 1,000	3	(22-34)
83	C		(37-55)	> 1,000	(12.5-14.4)	> 1,000	3	(37-50)
84	C		(46-65)	> 1,000	(75-101)	> 1,000	<1	(176-317)
*28	N		(48-96)	> 1,000 <sup>28</sup>	(7-21)	> 1,000 <sup>28</sup>	11	(82-95)
*30	N		(180-226)	> 1000 <sup>28</sup>	(4.6-6.5)	> 1,000 <sup>28</sup>	67	(29-51)

<sup>a</sup>The data are expressed as the geometric mean with 95% confidence limits in parentheses and derived from inhibition binding experiments and cAMP assays as described in the Experimental Section. <sup>b</sup>Displacement of specific [<sup>3</sup>H]DPCPX binding to hA<sub>1</sub>ARs ( $n = 3-6$ ). <sup>c</sup>Displacement of specific [<sup>3</sup>H]ZM241385 binding to hA<sub>2A</sub>ARs ( $n = 3-6$ ). <sup>d</sup>Displacement of [<sup>3</sup>H]MRE2029-F20 binding to hA<sub>2B</sub>ARs ( $n = 3-6$ ). <sup>e</sup>Displacement of specific [<sup>3</sup>H]MRE3008 F20 binding to hA<sub>3</sub>ARs ( $n = 3-6$ ). Data are expressed as geometric means with 95% confidence limits. <sup>f</sup>\*: Numbered in the Supporting Information.

(58). Purification by crystallization from dioxane/water. Yield 52%; mp 299 °C.

<sup>1</sup>H NMR (200 MHz, DMSO-*d*<sub>6</sub>):  $\delta$  0.85–0.92 (m, 6H), 1.58 (q,  $J = 7.2$  Hz, 2H), 1.75 (q,  $J = 7.2$  Hz, 2H), 3.85 (t,  $J = 7.0$  Hz, 2H), 4.00 (t,  $J = 7.2$  Hz, 2H), 4.09 (s, 3H), 5.37 (s, 2H), 6.66 (s, 1H), 7.22–7.80 (m, 3H), 12.95 (bs, 1H), 12.99 (bs, 1H). MS  $m/z$  541 (M H<sup>+</sup>). Anal. (C<sub>23</sub>H<sub>23</sub>BrN<sub>8</sub>O<sub>3</sub>) C, H, N.

**8-(1-Methyl-3-[[5-(trifluoromethyl)-1H-benzimidazol-2-yl]-methoxy]-1H-pyrazol-5-yl)-1,3-dipropyl-3,7-dihydro-1H-purine-2,6-dione (59)**. Purification by using column chromatography (ethyl acetate). Yield 50%; mp 299 °C.

<sup>1</sup>H NMR (200 MHz, DMSO-*d*<sub>6</sub>):  $\delta$  0.83–0.92 (m, 6H), 1.57 (q,  $J = 7.0$  Hz, 2H), 1.71 (q,  $J = 6.8$  Hz, 2H), 3.82 (t,  $J = 7.2$  Hz, 2H), 3.89 (t,

$J = 6.6$  Hz, 2H), 4.09 (s, 3H), 5.44 (s, 2H), 6.55 (s, 1H), 7.50–8.00 (m, 3H), 13.00 (bs, 1H), 13.99 (bs, 1H). MS  $m/z$  531 (M H<sup>+</sup>). Anal. (C<sub>24</sub>H<sub>25</sub>F<sub>3</sub>N<sub>8</sub>O<sub>3</sub>) C, H, N.

**8-(1-Methyl-3-[[5-methyl-1H-benzimidazol-2-yl]methoxy]-1H-pyrazol-5-yl)-1,3-dipropyl-3,7-dihydro-1H-purine-2,6-dione (60)**. Purification by using column chromatography (ethyl acetate). Yield 86%; mp 276 °C.

<sup>1</sup>H NMR (200 MHz, DMSO-*d*<sub>6</sub>):  $\delta$  0.830.92 (m, 6H), 1.57 (q,  $J = 7.2$  Hz, 2H), 1.73 (q,  $J = 7.2$  Hz, 2H), 2.4 (s, 3H), 3.86 (t,  $J = 7.2$  Hz, 2H), 4.00 (t,  $J = 7.2$  Hz, 2H), 4.10 (s, 3H), 5.33 (s, 2H), 6.48 (s, 1H), 6.93–7.00 (m, 1H), 7.27–7.49 (m, 2H), 12.5 (bs, 1H), 13.96 (bs, 1H). MS  $m/z$  477 (M H<sup>+</sup>). Anal. (C<sub>24</sub>H<sub>28</sub>N<sub>8</sub>O<sub>3</sub>) C, H, N.

**8-[1-Methyl-3-(1H-naphtho[2,3-d]imidazol-2-ylmethoxy)-1H-pyrazol-5-yl]-1,3-dipropyl-3,7-dihydro-1H-purine-2,6-dione (61).** Purification by crystallization from DMF. Yield 85%; mp 297 °C. <sup>1</sup>H NMR (200 MHz, DMSO-*d*<sub>6</sub>): δ 0.83–0.92 (m, 6H), 1.55 (q, *J* = 7.2 Hz, 2H), 1.71 (q, *J* = 7.0 Hz, 2H), 3.86 (t, *J* = 7.0 Hz, 2H), 4.00 (t, *J* = 7.0 Hz, 2H), 4.10 (s, 3H), 5.47 (s, 2H), 6.58 (s, 1H), 7.35–7.39 (m, 2H), 7.97–8.16 (m, 4H), 12.73 (bs, 1H), 13.98 (bs, 1H). MS *m/z* 513 (M H<sup>+</sup>). Anal. (C<sub>27</sub>H<sub>28</sub>N<sub>8</sub>O<sub>3</sub>) C, H, N.

**8-[1-Methyl-3-[(6-nitro-1H-benzimidazol-2-yl)methoxy]-1H-pyrazol-5-yl]-1,3-dipropyl-3,7-dihydro-1H-purine-2,6-dione (62).** Purification by crystallization from dioxane. Yield 58%; mp 263 °C.

<sup>1</sup>H NMR (400 MHz, DMSO-*d*<sub>6</sub>): δ 0.85–0.90 (m, 6H), 1.57 (q, *J* = 7.6 Hz, 2H), 1.72 (q, *J* = 7.2 Hz, 2H), 3.86 (t, *J* = 7.0 Hz, 2H), 3.99 (t, *J* = 7.8 Hz, 2H), 4.01 (s, 3H), 5.49 (s, 2H), 6.57 (s, 1H), 7.75 (d, *J* = 8.8 Hz, 1H), 8.13 (dd, *J*<sub>1</sub> = 8.8, *J*<sub>2</sub> = 2.4, Hz, 1H), 8.48 (d, *J* = 2.0 Hz, 1H), 12.95 (bs, 1H), 14.00 (bs, 1H). MS *m/z* 508 (M H<sup>+</sup>). Anal. (C<sub>23</sub>H<sub>23</sub>N<sub>8</sub>O<sub>3</sub>) C, H, N.

**2-[[5-(2,6-Dioxo-1,3-dipropyl-2,3,6,7-tetrahydro-1H-purin-8-yl)-1-methyl-1H-pyrazol-3-yl]oxy]methyl-1H-benzimidazole-5-carboxylic Acid Ethyl Ester (63).** Purification by crystallization from methanol. Yield 63%; mp >300 °C.

<sup>1</sup>H NMR (200 MHz, DMSO-*d*<sub>6</sub>): δ 0.83–0.92 (m, 6H), 1.32 (t, *J* = 7.0 Hz, 3H), 1.55 (q, *J* = 7.4 Hz, 2H), 1.72 (q, *J* = 7.2 Hz, 2H), 3.86 (t, *J* = 7.4 Hz, 2H), 3.97 (t, *J* = 7.6 Hz, 2H), 4.10 (s, 3H), 4.34 (q, *J* = 7.2 Hz, 2H), 5.42 (s, 2H), 6.53 (s, 1H), 7.76–8.22 (m, 3H), 13.00 (bs, 1H), 13.99 (bs, 1H). MS *m/z* 535 (M H<sup>+</sup>). Anal. (C<sub>26</sub>H<sub>30</sub>N<sub>8</sub>O<sub>5</sub>) C, H, N.

**2-[[5-(2,6-Dioxo-1,3-dipropyl-2,3,6,7-tetrahydro-1H-purin-8-yl)-1-methyl-1H-pyrazol-3-yl]oxy]methyl-1H-benzimidazole-5-carboxylic Acid (64).** The ester **63** (0.15 mmol) was dissolved in a mixture of 2:1 MeOH/10% NaOH. The solution was stirred at 50 °C for 3 h. The MeOH was evaporated, and the aqueous solution was acidified to pH 4–5 by using 10% HCl. The precipitate formed was collected by filtration, washed with water, and air-dried under vacuum to yield the corresponding carboxylic acid **64**, which was purified by crystallization (dioxane). Yield, 68%; mp >300 °C.

<sup>1</sup>H NMR (200 MHz, DMSO-*d*<sub>6</sub>): δ 0.83–0.92 (m, 6H), 1.33 (q, *J* = 7.0 Hz, 2H), 1.77 (q, *J* = 7.2 Hz, 2H), 4.01 (t, *J* = 7.0 Hz, 2H), 4.05 (t, *J* = 7.2 Hz, 2H), 4.10 (s, 3H), 5.41 (s, 2H), 6.66 (s, 1H), 7.82–8.20 (m, 3H), 12.99 (s, 1H), 13.00 (bs, 1H), 13.99 (bs, 1H). MS *m/z* 507 (M H<sup>+</sup>). Anal. (C<sub>24</sub>H<sub>26</sub>N<sub>8</sub>O<sub>5</sub>) C, H, N.

**8-[1-Methyl-3-[(4-methyl-1H-benzimidazol-2-yl)methoxy]-1H-pyrazol-5-yl]-1,3-dipropyl-3,7-dihydro-1H-purine-2,6-dione(65).** Purification by using column chromatography (ethyl acetate–methanol 9.5:0.5). Yield 86%; mp 276–277 °C.

<sup>1</sup>H NMR (200 MHz, DMSO-*d*<sub>6</sub>): δ 0.83–0.92 (m, 6H), 1.57 (q, *J* = 7.2 Hz, 2H), 1.73 (q, *J* = 7.4 Hz, 2H), 2.41 (s, 3H), 3.86 (t, *J* = 6.6 Hz, 2H), 3.98 (t, *J* = 7.4 Hz, 2H), 4.12 (s, 3H), 5.33 (s, 2H), 6.54 (s, 1H), 6.99–7.32 (m, 3H), 12.58 (bs, 1H), 13.97 (bs, 1H). MS *m/z* 477 (M H<sup>+</sup>). Anal. (C<sub>24</sub>H<sub>28</sub>N<sub>8</sub>O<sub>3</sub>) C, H, N.

**8-[1-Methyl-3-[(4-chloro-6-(trifluoromethyl)-1H-benzimidazol-2-yl)methoxy]-1H-pyrazol-5-yl]-1,3-dipropyl-3,7-dihydro-1H-purine-2,6-dione (66).** Purification by crystallization from methanol. Yield 48%; mp 267 °C.

<sup>1</sup>H NMR (200 MHz, DMSO-*d*<sub>6</sub>): δ 0.81–0.91 (m, 6H), 1.55 (q, *J* = 7.4 Hz, 2H), 1.72 (q, *J* = 7.2 Hz, 2H), 3.83 (t, *J* = 7.2 Hz, 2H), 3.96 (t, *J* = 7.4 Hz, 2H), 4.09 (s, 3H), 5.48 (s, 2H), 6.55 (s, 1H), 7.63 (s, 1H), 7.86 (s, 1H), 13.50 (bs, 1H), 14.00 (bs, 1H). MS *m/z* 565 (M H<sup>+</sup>). Anal. (C<sub>24</sub>H<sub>24</sub>ClF<sub>3</sub>N<sub>8</sub>O<sub>3</sub>) C, H, N.

**8-[3-[[4,6-Bis(trifluoromethyl)-1H-benzimidazol-2-yl]methoxy]-1-methyl-1H-pyrazol-5-yl]-1,3-dipropyl-3,7-dihydro-1H-purine-2,6-dione (67).** Purification by crystallization from methanol. Yield 55%; mp 281 °C.

<sup>1</sup>H NMR (200 MHz, DMSO-*d*<sub>6</sub>): δ 0.83–0.92 (m, 6H), 1.59 (q, *J* = 7.2 Hz, 2H), 1.78 (q, *J* = 7.0 Hz, 2H), 3.93 (t, *J* = 7.4 Hz, 2H), 4.09 (t, *J* = 7.0 Hz, 2H), 4.10 (s, 3H), 5.51 (s, 2H), 6.51 (s, 1H), 7.90 (s, 1H), 8.20 (s, 1H), 13.55 (bs, 1H), 14.00 (bs, 1H). MS *m/z* 599 (M H<sup>+</sup>). Anal. (C<sub>25</sub>H<sub>24</sub>F<sub>6</sub>N<sub>8</sub>O<sub>3</sub>) C, H, N.

**8-[3-[[5,6-Dichloro-1H-benzimidazol-2-yl)methoxy]-1-methyl-1H-pyrazol-5-yl]-1,3-dipropyl-3,7-dihydro-1H-purine-2,6-**

**dione (68).** Purification by crystallization from dioxane. Yield 55%; mp 288 °C.

<sup>1</sup>H NMR (200 MHz, DMSO-*d*<sub>6</sub>): δ 0.83–0.92 (m, 6H), 1.55 (q, *J* = 7.4 Hz, 2H), 1.78 (q, *J* = 7.2 Hz, 2H), 3.84 (t, *J* = 6.6 Hz, 2H), 3.99 (t, *J* = 7.0 Hz, 2H), 4.07 (s, 3H), 5.35 (s, 2H), 6.50 (s, 1H), 7.88 (s, 2H), 13.00 (bs, 1H), 14.00 (bs, 1H). MS *m/z* 515 (M H<sup>+</sup>). Anal. (C<sub>23</sub>H<sub>24</sub>Cl<sub>2</sub>N<sub>8</sub>O<sub>3</sub>) C, H, N.

**8-[3-[[5,6-Dimethyl-1H-benzimidazol-2-yl)methoxy]-1-methyl-1H-pyrazol-5-yl]-1,3-dipropyl-3,7-dihydro-1H-purine-2,6-dione (69).** Purification by crystallization from methanol. Yield 75%; mp 281 °C.

<sup>1</sup>H NMR (200 MHz, DMSO-*d*<sub>6</sub>): δ 0.83–0.92 (m, 6H), 1.58 (q, *J* = 7.2 Hz, 2H), 1.70 (q, *J* = 7.4 Hz, 2H), 2.29 (s, 6H), 3.84 (t, *J* = 6.8 Hz, 2H), 4.00 (t, *J* = 7.0 Hz, 2H), 4.10 (s, 3H), 5.31 (s, 2H), 6.53 (s, 1H), 7.30 (s, 2H), 12.45 (bs, 1H), 14.00 (bs, 1H). MS *m/z* 491 (M H<sup>+</sup>). Anal. (C<sub>25</sub>H<sub>30</sub>N<sub>8</sub>O<sub>3</sub>) C, H, N.

**8-[3-(1H-Benzimidazol-2-ylmethoxy)isoxazol-5-yl]-1,3-dipropyl-3,7-dihydro-1H-purine-2,6-dione (70).** Purification by crystallization from methanol. Yield 70%; mp 282 °C.

<sup>1</sup>H NMR (200 MHz, DMSO-*d*<sub>6</sub>): δ 0.85–0.92 (m, 6H), 1.58 (q, *J* = 7.2 Hz, 2H), 1.80 (q, *J* = 7.6 Hz, 2H), 3.98 (t, *J* = 7.2 Hz, 2H), 4.10 (t, *J* = 7.8 Hz, 2H), 5.53 (s, 2H), 6.97 (s, 1H), 7.20–7.59 (m, 4H), 12.76 (bs, 1H), 14.59 (bs, 1H). MS *m/z* 450 (M H<sup>+</sup>). Anal. (C<sub>22</sub>H<sub>23</sub>N<sub>7</sub>O<sub>4</sub>) C, H, N.

**8-[3-[[5-Chloro-1H-benzimidazol-2-yl)methoxy]isoxazol-5-yl]-1,3-dipropyl-3,7-dihydro-1H-purine-2,6-dione (71).** Purification by crystallization from methanol. Yield 68%; mp 260 °C.

<sup>1</sup>H NMR (200 MHz, DMSO-*d*<sub>6</sub>): δ 0.83–0.92 (m, 6H), 1.55 (q, *J* = 7.6 Hz, 2H), 1.70 (q, *J* = 7.2 Hz, 2H), 3.86 (t, *J* = 7.4 Hz, 2H), 3.94 (t, *J* = 7.2 Hz, 2H), 5.54 (s, 2H), 6.99 (s, 1H), 7.20–7.77 (m, 3H), 13.00 (bs, 1H), 14.55 (bs, 1H). MS *m/z* 484 (M H<sup>+</sup>). Anal. (C<sub>22</sub>H<sub>22</sub>ClN<sub>7</sub>O<sub>4</sub>) C, H, N.

**8-[3-[[5-Bromo-1H-benzimidazol-2-yl)methoxy]isoxazol-5-yl]-1,3-dipropyl-3,7-dihydro-1H-purine-2,6-dione (72).** Purification by crystallization from methanol. Yield 70%; mp 230 °C.

<sup>1</sup>H NMR (200 MHz, DMSO-*d*<sub>6</sub>): δ 0.82–0.92 (m, 6H), 1.58 (q, *J* = 7.6 Hz, 2H), 1.72 (q, *J* = 7.2 Hz, 2H), 3.89 (t, *J* = 7.2 Hz, 2H), 3.98 (t, *J* = 7.4 Hz, 2H), 5.54 (s, 2H), 6.98 (s, 1H), 7.36–7.80 (m, 3H), 13.00 (bs, 1H), 14.60 (bs, 1H). MS *m/z* 529 (M H<sup>+</sup>). Anal. (C<sub>22</sub>H<sub>22</sub>BrN<sub>7</sub>O<sub>4</sub>) C, H, N.

**1,3-Dipropyl-8-(3-[[5-(trifluoromethyl)-1H-benzimidazol-2-yl]methoxy]isoxazol-5-yl)-3,7-dihydro-1H-purine-2,6-dione (73).** Purification by crystallization from methanol. Yield 65%; mp 268 °C.

<sup>1</sup>H NMR (200 MHz, DMSO-*d*<sub>6</sub>): δ 0.83–0.92 (m, 6H), 1.55 (q, *J* = 7.6 Hz, 2H), 1.69 (q, *J* = 7.2 Hz, 2H), 3.86 (t, *J* = 7.6 Hz, 2H), 3.98 (t, *J* = 7.4 Hz, 2H), 5.61 (s, 2H), 7.00 (s, 1H), 7.66–8.00 (m, 3H), 13.20 (bs, 1H), 14.70 (bs, 1H). MS *m/z* 518 (M H<sup>+</sup>). Anal. (C<sub>23</sub>H<sub>22</sub>F<sub>3</sub>N<sub>7</sub>O<sub>4</sub>) C, H, N.

**8-[3-[[5-Methoxy-1H-benzimidazol-2-yl)methoxy]isoxazol-5-yl]-1,3-dipropyl-3,7-dihydro-1H-purine-2,6-dione (74).** Purification by crystallization from methanol. Yield 75%; mp 199 °C.

<sup>1</sup>H NMR (200 MHz, DMSO-*d*<sub>6</sub>): δ 0.83–0.92 (m, 6H), 1.59 (q, *J* = 7.6 Hz, 2H), 1.69 (q, *J* = 7.4 Hz, 2H), 3.78 (s, 3H), 3.86 (t, *J* = 7.8 Hz, 2H), 3.98 (t, *J* = 7.6 Hz, 2H), 5.48 (s, 2H), 6.86 (dd, *J*<sub>1</sub> = 8.8 Hz, *J*<sub>2</sub> = 2.2 Hz, 1H), 6.97 (s, 1H), 7.46 (d, *J* = 8.8 Hz, 1H), 13.01 (bs, 1H), 14.30 (bs, 1H). MS *m/z* 480 (M H<sup>+</sup>). Anal. (C<sub>23</sub>H<sub>25</sub>N<sub>7</sub>O<sub>5</sub>) C, H, N.

**8-[3-[[5-Chloro-6-fluoro-1H-benzimidazol-2-yl)methoxy]isoxazol-5-yl]-1,3-dipropyl-3,7-dihydro-1H-purine-2,6-dione (75).** Purification by crystallization from methanol. Yield 55%; mp 249 °C.

<sup>1</sup>H NMR (200 MHz, DMSO-*d*<sub>6</sub>): δ 0.86–0.92 (m, 6H), 1.55 (q, *J* = 7.2 Hz, 2H), 1.69 (q, *J* = 7.4 Hz, 2H), 3.88 (t, *J* = 7.6 Hz, 2H), 3.97 (t, *J* = 7.8 Hz, 2H), 5.54 (s, 2H), 6.98 (s, 1H), 7.65–7.80 (m, 2H), 13.06 (bs, 1H), 14.61 (bs, 1H). MS *m/z* 502 (M H<sup>+</sup>). Anal. (C<sub>23</sub>H<sub>21</sub>ClF<sub>2</sub>N<sub>7</sub>O<sub>4</sub>) C, H, N.

**8-[3-[[4-Chloro-6-(trifluoromethyl)-1H-benzimidazol-2-yl]methoxy]isoxazol-5-yl]-1,3-dipropyl-3,7-dihydro-1H-purine-2,6-dione (76).** Purification by crystallization from methanol. Yield 50%; mp 251 °C.

$^1\text{H}$  NMR (200 MHz, DMSO- $d_6$ ):  $\delta$  0.86–0.92 (m, 6H), 1.59 (q,  $J$  = 7.4 Hz, 2H), 1.69 (q,  $J$  = 7.2 Hz, 2H), 3.86 (t,  $J$  = 7.0 Hz, 2H), 3.97 (t,  $J$  = 7.2 Hz, 2H), 5.96 (s, 2H), 6.95 (s, 1H), 7.48 (s, 1H), 7.98 (s, 1H), 10.00 (bs, 1H), 14.20 (bs, 1H). MS  $m/z$  552 (M  $\text{H}^+$ ). Anal. ( $\text{C}_{23}\text{H}_{21}\text{ClF}_3\text{N}_7\text{O}_4$ ) C, H, N.

**8-(3-[[4,6-Bis(trifluoromethyl)-1H-benzimidazol-2-yl]-methoxy]isoxazol-5-yl)-1,3-dipropyl-3,7-dihydro-1H-purine-2,6-dione (77).** Purification by crystallization from methanol. Yield 60%; mp 233 °C.

$^1\text{H}$  NMR (200 MHz, DMSO- $d_6$ ):  $\delta$  0.81–0.91 (m, 6H), 1.52 (q,  $J$  = 7.4 Hz, 2H), 1.67 (q,  $J$  = 8.0 Hz, 2H), 3.86 (t,  $J$  = 7.0 Hz, 2H), 3.94 (t,  $J$  = 6.8 Hz, 2H), 5.64 (s, 2H), 6.68 (s, 1H), 7.84 (s, 1H), 8.26 (s, 1H), 13.06 (bs, 1H), 14.00 (bs, 1H). MS  $m/z$  586 (M  $\text{H}^+$ ). Anal. ( $\text{C}_{24}\text{H}_{21}\text{F}_6\text{N}_7\text{O}_4$ ) C, H, N.

**8-[1-Methyl-3-(7H-purin-8-ylmethoxy)-1H-pyrazol-5-yl]-1,3-dipropyl-3,7-dihydro-1H-purine-2,6-dione (78).** The same procedure as reported for the preparation of compounds 54–69, except a temperature of 100 °C was necessary for the ring closure of the amide intermediate.

Purification by crystallization from DMF/water. Yield 60%; mp 293–294 °C.

$^1\text{H}$  NMR (200 MHz, DMSO- $d_6$ ):  $\delta$  0.80–0.89 (m, 6H), 1.54 (q,  $J$  = 7.6 Hz, 2H), 1.70 (q,  $J$  = 7.2 Hz, 2H), 3.83 (t,  $J$  = 7.2 Hz, 2H), 3.97 (t,  $J$  = 7.2 Hz, 2H), 4.05 (s, 3H), 5.44 (s, 2H), 6.50 (s, 1H), 8.87 (s, 1H), 9.03 (s, 1H), 13.77 (bs, 2H). MS  $m/z$  465 (M  $\text{H}^+$ ). Anal. ( $\text{C}_{21}\text{H}_{24}\text{N}_{10}\text{O}_3$ ) C, H, N.

**8-(3-[[5-(3-Methoxyphenyl)-1,2,4-oxadiazol-3-yl]methoxy]-1-methyl-1H-pyrazol-5-yl)-1,3-dipropyl-3,7-dihydro-1H-purine-2,6-dione (79).** The SEM protected X (50 mg, 0.07 mmol) was dissolved in ethanol (2 mL) and treated with HCl 1N (0.5 mL) for 4 h at 80 °C. After cooling to room temperature, the precipitate formed was filtered and washed with ethanol to afford pure 79. Yield 85%; mp 242 °C.

$^1\text{H}$  NMR (200 MHz, DMSO- $d_6$ ):  $\delta$  0.83–0.92 (m, 6H), 1.55 (q,  $J$  = 7.8 Hz, 2H), 1.73 (q,  $J$  = 7.8 Hz, 2H), 3.87 (s, 3H), 3.89 (t,  $J$  = 7.2 Hz, 2H), 4.01 (t,  $J$  = 7.6 Hz, 2H), 4.09 (s, 3H), 5.40 (s, 2H), 6.53 (s, 1H), 7.31–7.74 (m, 4H), 13.98 (bs, 1H). MS  $m/z$  521 (M  $\text{H}^+$ ). Anal. ( $\text{C}_{23}\text{H}_{28}\text{N}_8\text{O}_5$ ) C, H, N.

**8-(3-Hydroxy-1-methyl-1H-pyrazol-5-yl)-1,3-dipropyl-3,7-dihydro-1H-purine-2,6-dione (80).** The same procedure as reported for the preparation of compound VIII, except used VI. Yield 80%; mp >300 °C.

$^1\text{H}$  NMR (200 MHz, DMSO- $d_6$ ):  $\delta$  0.83–0.92 (m, 6H), 1.58 (q,  $J$  = 7.2 Hz, 2H), 1.75 (q,  $J$  = 7.8 Hz, 2H), 3.86 (t,  $J$  = 7.6 Hz, 2H), 3.89 (t,  $J$  = 8.0 Hz, 2H), 4.04 (s, 3H), 6.25 (s, 1H), 9.95 (s, 1H), 13.80 (bs, 1H). MS  $m/z$  333 (M  $\text{H}^+$ ). Anal. ( $\text{C}_{15}\text{H}_{20}\text{N}_6\text{O}_3$ ) C, H, N.

**6-(3-Hydroxy-1-methyl-1H-pyrazol-5-yl)-1,3-dipropyl-1H-pyrrolo[3,2-d]pyrimidine-2,4(3H,5H)-dione (81).** Same procedure as for compound VIII except used XIV. Yield 80%; mp 282 °C.  $^1\text{H}$  NMR (DMSO- $d_6$ ):  $\delta$  0.87 (m, 6H), 1.62 (m, 2H), 3.76 (s, 3H), 3.85 (m, 4H), 5.96 (s, 2H), 6.51 (s, 1H), 9.77 (bs, 1H), 12.3 (bs, 1H). MS  $m/z$  332 (M  $\text{H}^+$ ). Anal. ( $\text{C}_{16}\text{H}_{21}\text{N}_5\text{O}_3$ ) C, H, N.

**6-[3-(1H-Benzimidazol-2-ylmethoxy)-1-methyl-1H-pyrazol-5-yl]-1,3-dipropyl-1H-pyrrolo[3,2-d]pyrimidine-2,4(3H,5H)-dione (82).** The same procedure as for compound 54 except used XIX. Yield 85%; mp 224 °C.  $^1\text{H}$  NMR (200 MHz, DMSO- $d_6$ ):  $\delta$  0.82–0.93 (m, 6H), 1.60–1.75 (m, 4H), 3.86 (s, 3H), 3.89–3.99 (m, 4H), 5.34 (s, 2H), 6.26 (s, 1H), 6.55 (s, 1H), 7.20–7.62 (m, 4H), 12.50 (bs, 1H), 12.65 (bs, 1H). MS  $m/z$  462 (M  $\text{H}^+$ ). Anal. ( $\text{C}_{24}\text{H}_{27}\text{N}_7\text{O}_3$ ) C, H, N.

**Preparation of 2-[[5-(2,4-Dioxo-1,3-dipropyl-2,3,4,5-tetrahydro-1H-pyrrolo[3,2-d]pyrimidin-6-yl)-1-methyl-1H-pyrazol-3-yl]oxy]-N-(4-fluorophenyl)acetamide (83) and N-1,3-Benzodioxol-5-yl-2-[[5-(2,4-dioxo-1,3-dipropyl-2,3,4,5-tetrahydro-1H-pyrrolo[3,2-d]pyrimidin-6-yl)-1-methyl-1H-pyrazol-3-yl]oxy]acetamide (84).** To a mixture of the carboxylic acid XIX (0.15 mmol), EDC (0.15 mmol), and anhydrous DMF (5 mL) was added the appropriate aniline (0.15 mmol), and the mixture was stirred at room temperature for 5 h under argon atmosphere. The resulting solution was evaporated under reduced pressure, and treated with water. The precipitate formed was collected by filtration and washed

with water. The resulting crude was purified by column chromatography (ethyl acetate–methanol 9:1).

**83.** Yield 65%; mp 215 °C.  $^1\text{H}$  NMR (200 MHz, DMSO- $d_6$ ):  $\delta$  0.82–0.93 (m, 6H), 1.52–1.65 (m, 4H), 3.82 (s, 3H), 3.86–3.99 (m, 4H), 4.73 (s, 2H), 6.24 (s, 1H), 6.57 (s, 1H), 7.15–7.20 (m, 2H), 7.61–7.66 (m, 2H), 10.15 (bs, 1H), 12.40 (bs, 1H). MS  $m/z$  483 (M  $\text{H}^+$ ). Anal. ( $\text{C}_{24}\text{H}_{27}\text{FN}_6\text{O}_4$ ) C, H, N.

**84.** Yield 60%; mp: 226 °C.  $^1\text{H}$  NMR (200 MHz, DMSO- $d_6$ ):  $\delta$  0.86 (m, 6H), 1.62 (m, 4H), 3.82 (s, 3H), 3.86 (m, 4H), 4.70 (s, 2H), 5.98 (s, 2H), 6.23 (s, 1H), 6.56 (s, 1H), 6.85 (d,  $J$  = 8.4 Hz 1H), 7.00 (d,  $J$  = 8.4 Hz 1H), 7.32 (s, 1H), 9.99 (s, 1H), 12.44 (s, 1H). MS  $m/z$  509 (M  $\text{H}^+$ ). Anal. ( $\text{C}_{25}\text{H}_{28}\text{N}_6\text{O}_6$ ) C, H, N.

**Determination of Affinity ( $K_i$ ) and Potency ( $\text{IC}_{50}$ ) Values of the Novel Adenosine Compounds.** Cell membranes preparation. The human ARs have been transfected in CHO or HEK293 cells according with the method previously described.<sup>36,37</sup> Briefly, the cells were grown adherently and maintained in Dulbecco's Modified Eagles Medium (DMEM) with nutrient mixture F12 (DMEM/F12) without nucleosides, containing 10% fetal calf serum, penicillin (100 U/mL), streptomycin (100  $\mu\text{g}/\text{mL}$ ), L-glutamine (2 mM), and Geneticin (G418, 0.2 mg/mL) at 37 °C in 5%  $\text{CO}_2/95\%$  air. For membrane preparation the culture medium was removed and the cells were washed with phosphate-buffered saline and scraped off T75 flasks in ice-cold suspension tonic buffer (5 mM Tris HCl, 1 mM EDTA, pH 7.4). The cell suspension was homogenized with Polytron, the homogenate was spun for 10 min at 1000g, and the supernatant was then centrifuged for 30 min at 100000g. The membrane pellet was suspended in 50 mM Tris HCl buffer (pH 7.4) for  $\text{A}_1\text{ARs}$ , in 50 mM Tris HCl, 10 mM  $\text{MgCl}_2$  (pH 7.4) for  $\text{A}_{2A}\text{ARs}$ , in 50 mM Tris HCl, 10 mM  $\text{MgCl}_2$ , 1 mM EDTA (pH 7.4) for  $\text{A}_{2B}$  and  $\text{A}_3\text{ARs}$ .

**Competition Binding Experiments to Human  $\text{A}_1$ ,  $\text{A}_{2A}$ ,  $\text{A}_{2B}$ , and  $\text{A}_3\text{ARs}$ .** All new synthesized compounds have been tested to evaluate their affinity to human  $\text{A}_1$ ,  $\text{A}_{2A}$ ,  $\text{A}_{2B}$ , and  $\text{A}_3\text{ARs}$ . Displacement experiments of [ $^3\text{H}$ ]-DPCPX (1,3-[ $^3\text{H}$ ]-dipropyl-8-cyclopentylxanthine) to CHO cells transfected with the human recombinant  $\text{A}_1\text{ARs}$  were carried out for 120 min at 25 °C incubating diluted membranes (50  $\mu\text{g}$  of protein/assay) and at least 6–8 different concentrations of examined antagonists.<sup>38</sup> Nonspecific binding was determined in the presence of DPCPX 10  $\mu\text{M}$ , and this was always  $\leq 10\%$  of the total binding. Binding of [ $^3\text{H}$ ]-ZM 241385 (4-(2-[7-amino-2-(2-furyl)[1,2,4]-triazolo[2,3-a][1,3,5]triazin-5-ylamino]-ethyl)phenol) to CHO cells transfected with the human recombinant  $\text{A}_{2A}\text{ARs}$  was performed by using a suspension of membranes (50  $\mu\text{g}$  of protein/assay) and at least 6–8 different concentrations of studied antagonists for an incubation time of 60 min at 4 °C.<sup>39</sup> Nonspecific binding was determined in the presence of 1  $\mu\text{M}$  ZM 241385 and was about 20% of total binding. Competition binding experiments of tritiated-30 to HEK293 cells transfected with the human recombinant  $\text{A}_{2B}\text{ARs}$  were carried out incubating for 120 min at 4 °C diluted membranes (50  $\mu\text{g}$  of protein/assay) and at least 6–8 different concentrations of examined compounds.<sup>40</sup> Nonspecific binding was defined as binding in the presence of 1  $\mu\text{M}$  MRE 2029F20 and was about 25% of total binding. Inhibition binding assays of [ $^3\text{H}$ ]-MRE 3008F20 (5-N-(4-methoxyphenylcarbamoyl)amino-8-propyl-2-(2-furyl)pyrazolo[4,3-e]-1,2,4-triazolo[1,5-c]pyrimidine) in CHO cells transfected with the human recombinant  $\text{A}_3\text{ARs}$  were performed incubating for 120 min at 4 °C diluted membranes (50  $\mu\text{g}$  of protein/assay) and at least 6–8 different concentrations of examined ligands.<sup>41</sup> Bound and free radioactivity was separated by filtering the assay mixture through Whatman GF/B glass fiber filters using a Brandel cell harvester (Brandel Instruments, Unterföhring, Germany). The filter-bound radioactivity was counted by a Packard Tri Carb 2810 TR (Perkin-Elmer) scintillation counter.

**Measurement of Cyclic AMP Levels in CHO Cells Transfected with Human  $\text{A}_{2B}\text{ARs}$ .** CHO cells transfected with human  $\text{A}_{2B}\text{ARs}$  were washed with phosphate-buffered saline, diluted trypsinase, and centrifuged for 10 min at 200g. The pellet resulting was suspended in 0.5 mL of incubation mixture: NaCl 150 mM, KCl 2.7 mM,  $\text{NaH}_2\text{PO}_4$  0.37 mM,  $\text{MgSO}_4$  1 mM,  $\text{CaCl}_2$  1 mM, Hepes 5 mM,  $\text{MgCl}_2$  10 mM, glucose 5 mM, pH 7.4 at 37 °C. Then 2.0 IU/mL

adenosine deaminase and 0.5 mM 4-(3-butoxy-4-methoxybenzyl)-2-imidazolidinone (Ro 20-1724) as phosphodiesterase inhibitor were added and preincubated for 10 min in a shaking bath at 37 °C.<sup>41</sup> The potencies of antagonists studied were determined by antagonism of NECA (100 nM)-induced stimulation of cyclic AMP levels. The reaction was terminated by the addition of cold 6% trichloroacetic acid (TCA). The TCA suspension was centrifuged at 2000g for 10 min at 4 °C, and the supernatant was extracted four times with water saturated diethyl ether. The final aqueous solution was tested for cyclic AMP levels by a competition protein binding assay. Samples of cyclic AMP standard (0–10 pmoles) were added to each test tube containing the incubation buffer (trizma base 0.1 M, aminophylline 8.0 mM, 2 mercaptoethanol 6.0 mM, pH 7.4) and [<sup>3</sup>H] cyclic AMP in a total volume of 0.5 mL. The binding protein previously prepared from beef adrenals, was added to the samples previously incubated at 4 °C for 150 min, and after the addition of charcoal were centrifuged at 2000g for 10 min. The clear supernatant was counted with 4 mL of Atomlight liquid scintillator and counted in a Tri Carb 2810 TR (Perkin-Elmer) scintillation counter.

**Data Analysis.** The protein concentration was determined according to a Bio-Rad method<sup>42</sup> with bovine albumin as a standard reference. Inhibitory binding constant,  $K_i$ , values were calculated from those of  $IC_{50}$  according to Cheng and Prusoff equation  $K_i = IC_{50}/(1 + [C^*]/K_D^*)$ , where  $[C^*]$  is the concentration of the radioligand and  $K_D^*$  its dissociation constant.<sup>43</sup> In addition, a weighted nonlinear least-squares curve fitting program LIGAND was used for computer analysis of the inhibition binding experiments.<sup>44</sup> The  $IC_{50}$  values obtained in cyclic AMP assays were calculated by nonlinear regression analysis using the equation for a sigmoidal concentration response curves (Graph Pad Prism, San Diego, CA). All experimental data are expressed as the geometric mean with 95% confidence limits in parentheses of three or four independent experiments performed in duplicate.

## ■ ASSOCIATED CONTENT

### ■ Supporting Information

Additional synthetic, spectroscopic, analytical, and molecular modeling data. This material is available free of charge via the Internet at <http://pubs.acs.org>.

## ■ AUTHOR INFORMATION

### Corresponding Author

\*For P.G.B.: phone, +39-0532-455921; fax, +39-0532-455921; E-mail, [baraldi@dns.unife.it](mailto:baraldi@dns.unife.it). For M.A.T.: phone, +39-0532-455926; fax, +39-0532-455921; E-mail, [tbj@dns.unife.it](mailto:tbj@dns.unife.it).

## ■ ACKNOWLEDGMENTS

We thank King Pharmaceuticals, Inc., Research and Development, 4000 CentreGreen Way, Suite 300, Cary, North Carolina 27513, for financial support.

## ■ ABBREVIATIONS USED

AR, adenosine receptor; cAMP, cyclic adenosine monophosphate; ADA, adenosine deaminase; CHO, Chinese hamster ovary; CoMFA, comparative molecular field analysis; COPD, chronic obstructive pulmonary disease; DMF, dimethylformamide; DMSO, dimethylsulfoxide; DMEM, Dulbecco's Modified Eagle Medium; EDC, *N*-(3-(dimethylamino)propyl)-*N'*-ethylcarbodiimide; HMC-1, human mast cell line; HEK, human embryonic kidney; h, human; MAPK, mitogen-activated protein kinase; IL, interleukin; mitogen-activated protein kinase; NECA, *S'*-*N*-ethylcarboxamidoadenosine; PCC, pyridinium chlorocromate; QSAR, quantitative structure–activity relationship; rmsd, root-mean-square deviation; mRNA, messenger ribonucleic acid; SEM-Cl, 2-(trimethylsilyl)-ethoxymethyl chloride

## ■ REFERENCES

- (1) Feoktistov, I.; Biaggioni, I. Adenosine  $A_{2B}$  receptors. *Pharmacol. Rev.* **1997**, *49*, 381–402.
- (2) Fredholm, B. B.; IJzerman, A. P.; Jacobson, K. A.; Klotz, K. N.; Linden, J. International Union of Pharmacology. XXV. Nomenclature and classification of adenosine receptors. *Pharmacol. Rev.* **2001**, *53*, 527–552.
- (3) Linden, J. Molecular approach to adenosine receptors: receptor-mediated mechanisms of tissue protection. *Annu. Rev. Pharmacol. Toxicol.* **2001**, *41*, 775–787.
- (4) Feoktistov, I.; Biaggioni, I. Adenosine  $A_{2B}$  receptors evoke interleukin-8 secretion in human mast cells. An enprofylline-sensitive mechanism with implications for asthma. *J. Clin. Invest.* **1995**, *96*, 1979–1986.
- (5) Hinschen, A. K.; Rose'Meyer, R. B.; Headrick, J. P. Adenosine receptor subtypes mediating coronary vasodilation in rat hearts. *J. Cardiovasc. Pharmacol.* **2003**, *41*, 73–80.
- (6) Morrison, R. R.; Talukder, M. A.; Ledent, C.; Mustafa, S. J. Cardiac effects of adenosine in  $A_{2A}$  receptor knockout hearts: uncovering  $A(2B)$  receptors. *Am. J. Physiol. Heart Circ. Physiol.* **2002**, *282*, H437–H444.
- (7) Wakeno, M.; Minamino, T.; Seguchi, O.; Okazaki, H.; Tsukamoto, O.; Okada, K.; Hirata, A.; Fujita, M.; Asanuma, H.; Kim, J.; Komamura, K.; Takashima, S.; Mochizuki, N.; Kitakaze, M. Long-term stimulation of adenosine  $A_{2B}$  receptors begun after myocardial infarction prevents cardiac remodeling in rats. *Circulation* **2006**, *114*, 1923–1932.
- (8) Philipp, S.; Yang, X. M.; Cui, L.; Davis, A. M.; Downey, J. M.; Cohen, M. V. Postconditioning protects rabbit hearts through a protein kinase C-adenosine  $A_{2B}$  receptor cascade. *Cardiovasc. Res.* **2006**, *70*, 308–314.
- (9) Strohmeier, G. R.; Reppert, S. M.; Lencer, W. I.; Madara, J. L. The  $A_{2B}$  adenosine receptor mediates cAMP responses to adenosine receptor agonists in human intestinal epithelia. *J. Biol. Chem.* **1995**, *270*, 2387–2394.
- (10) Strohmeier, G. R.; Lencer, W. I.; Patapoff, T. W.; Thompson, L. F.; Carlson, S. L.; Moe, S. J.; Carnes, D. K.; Mrsny, R. J.; Madara, J. L. Surface expression, polarization, and functional significance of CD73 in human intestinal epithelia. *J. Clin. Invest.* **1997**, *99*, 2588–2601.
- (11) Kolachala, V.; Asamoah, V.; Wang, L.; Obertone, T. S.; Ziegler, T. R.; Merlin, D.; Sitaraman, S. V. TNF-alpha upregulates adenosine  $2b$  ( $A_{2B}$ ) receptor expression and signaling in intestinal epithelial cells: a basis for  $A_{2B}R$  overexpression in colitis. *Cell. Mol. Life Sci.* **2005**, *62*, 2647–2657.
- (12) Bjorck, T.; Gustafsson, L. E.; Dahlen, S. E. Isolated bronchi from asthmatics are hyperresponsive to adenosine, which apparently acts indirectly by liberation of leukotrienes and histamine. *Am. Rev. Respir. Dis.* **1992**, *145*, 1087–1091.
- (13) Varani, K.; Caramori, G.; Vincenzi, F.; Adcock, I.; Casolari, P.; Leung, E.; MacLennan, S.; Gessi, S.; Morello, S.; Barnes, P. J.; Ito, K.; Chung, K. F.; Cavalleco, G.; Azzena, G.; Papi, A.; Borea, P. A. Alteration of adenosine receptors in patients with chronic obstructive pulmonary disease. *Am. J. Respir. Crit. Care Med.* **2006**, *173*, 398–406.
- (14) Spicuzza, L.; Di Maria, G.; Polosa, R. Adenosine in the airways: implications and applications. *Eur. J. Pharmacol.* **2006**, *533*, 77–88.
- (15) Polosa, R.; Rorke, S.; Holgate, S. T. Evolving concepts on the value of adenosine hyperresponsiveness in asthma and chronic obstructive pulmonary disease. *Thorax* **2002**, *57*, 649–654.
- (16) Feoktistov, I.; Polosa, R.; Holgate, S. T.; Biaggioni, I. Adenosine  $A_{2B}$  receptors: a novel therapeutic target in asthma? *Trends Pharmacol. Sci.* **1998**, *19*, 148–153.
- (17) Varani, K.; Caramori, G.; Vincenzi, F.; Tosi, A.; Barczyk, A.; Contoli, M.; Casolari, P.; Triggiani, M.; Hansel, T.; Leung, E.; MacLennan, S.; Barnes, P. J.; Chung, K. F.; Adcock, I.; Papi, A.; Borea, P. A. Oxidative/nitrosative stress selectively altered  $A_{2B}$  adenosine receptors in chronic obstructive pulmonary disease. *FASEB J.* **2010**, *24*, 1192–1204.
- (18) Sun, C. X.; Zhong, H.; Mohsenin, A.; Morschl, E.; Chunn, J. L.; Molina, J. G.; Belardinelli, L.; Zeng, D.; Blackburn, M. R. Role of  $A_{2B}$

adenosine receptor signaling in adenosine-dependent pulmonary inflammation and injury. *J. Clin. Invest.* **2006**, *116*, 2173–2182.

(19) Baraldi, P. G.; Aghazadeh Tabrizi, M.; Gessi, S.; Borea, P. A. Adenosine Receptor Antagonists: Translating Medicinal Chemistry and Pharmacology into Clinical Utility. *Chem. Rev.* **2008**, *108*, 238–263.

(20) Beukers, M. W.; Meurs, I.; IJzerman, A. P. Structure–affinity relationships of adenosine A<sub>2B</sub> receptor ligands. *Med. Res. Rev.* **2006**, *26*, 667–698.

(21) Kalla, R. V.; Zablocki, J.; Aghazadeh Tabrizi, M.; Baraldi, P. G. Recent Developments in A<sub>2B</sub> Adenosine Receptor Ligands. *Handb. Experi. Pharmacol.* **2009**, *193*, 99–122.

(22) Zablocki, J.; Elzein, E.; Kalla, R. A<sub>2B</sub> adenosine receptor antagonists and their potential indications. *Expert Opin. Ther. Pat.* **2006**, *16*, 1347–1357.

(23) Kim, S. A.; Marshall, M. A.; Melman, N.; Kim, H. S.; Muller, C. E.; Linden, J.; Jacobson, K. A. Structure–activity relationships at human and rat A<sub>2B</sub> adenosine receptors of xanthine derivatives substituted at the 1-, 3-, 7-, and 8-positions. *J. Med. Chem.* **2002**, *45*, 2131–2138.

(24) Zablocki, J.; Kalla, R.; Perry, T.; Palle, V.; Varkhedkar, V.; Xiao, D.; Piscopio, A.; Maa, T.; Gimbel, A.; Hao, J.; Chu, N.; Leung, K.; Zeng, D. The discovery of a selective, high affinity A<sub>2B</sub> adenosine receptor antagonist for the potential treatment of asthma. *Bioorg. Med. Chem. Lett.* **2005**, *15*, 609–612.

(25) Elzein, E.; Kalla, R. V.; Li, X.; Perry, T.; Gimbel, A.; Zeng, D.; Lustig, D.; Leung, K.; Zablocki, J. Discovery of a novel A<sub>2B</sub> adenosine receptor antagonist as a clinical candidate for chronic inflammatory airway diseases. *J. Med. Chem.* **2008**, *51*, 2267–2278.

(26) Eastwood, P.; Esteve, C.; Gonzalez, J.; Fonquerna, S.; Aiguade, J.; Carranco, I. S.; Domenech, T.; Aparici, M.; Miralpeix, M.; Alberti, J.; Cordoba, M.; Fernandez, R.; Pont, M.; Godessart, N.; Prats, N.; Loza, M. I.; Cadavid, M. I.; Nueda, A.; Vidal, B. Discovery of LAS101057: A Potent, Selective, and Orally Efficacious A<sub>2B</sub> Adenosine Receptor Antagonist. *Med. Chem. Lett.* **2011**, *2*, 213–218.

(27) Castelhan, A. L.; McKibben, B.; Steinig, A. G. Pyrrolopyrimidine A<sub>2B</sub> selective antagonist compound, their synthesis and use. WO Patent 3053361, 2003.

(28) Baraldi, P. G.; Tabrizi, M. A.; Preti, D.; Bovero, A.; Romagnoli, R.; Fruttarolo, F.; Zaid, N. A.; Moorman, A. R.; Varani, K.; Gessi, S.; Merighi, S.; Borea, P. A. Design, synthesis, and biological evaluation of new 8-heterocyclic xanthine derivatives as highly potent and selective human A<sub>2B</sub> adenosine receptor antagonists. *J. Med. Chem.* **2004**, *47*, 1434–1447.

(29) Baraldi, P. G.; Tabrizi, M. A.; Preti, D.; Bovero, A.; Fruttarolo, F.; Romagnoli, R.; Moorman, A. R.; Gessi, S.; Merighi, S.; Varani, K.; Borea, P. A. [<sup>3</sup>H]-MRE 2029-F20, a selective antagonist radioligand for the human A<sub>2B</sub> adenosine receptors. *Bioorg. Med. Chem. Lett.* **2004**, *14*, 3607–3610.

(30) Carotti, A.; Cadavid, M. I.; Centeno, N. B.; Esteve, C.; Loza, M. I.; Martinez, A.; Nieto, R.; Ravina, E.; Sanz, F.; Segarra, V.; Sotelo, E.; Stefanachi, A.; Vidal, B. Design, synthesis, and structure–activity relationships of 1-,3-,8-, and 9-substituted-9-deazaxanthines at the human A<sub>2B</sub> adenosine receptor. *J. Med. Chem.* **2006**, *49*, 282–299.

(31) Stefanachi, A.; Leonetti, F.; Cappa, A.; Carotti, A. Fast and highly efficient one-pot synthesis of 9-deazaxanthines. *Tetrahedron Lett.* **2003**, *44*, 2121–2123.

(32) Daly, J. W.; Padgett, W.; Shamim, M. T.; Butts-Lamb, P.; Waters, J. 1,3-Dialkyl-8-(*p*-sulfophenyl)xanthines: potent water-soluble antagonists for A<sub>1</sub>- and A<sub>2</sub>-adenosine receptors. *J. Med. Chem.* **1985**, *28*, 487–492.

(33) Elzein, E.; Kalla, R.; Li, X.; Perry, T.; Parkhill, E.; Palle, V.; Varkhedkar, V.; Gimbel, A.; Zeng, D.; Lustig, D.; Leung, K.; Zablocki, J. Novel 1,3-dipropyl-8-(1-heteroaryl-methyl-1*H*-pyrazol-4-yl)-xanthine derivatives as high affinity and selective A<sub>2B</sub> adenosine receptor antagonists. *Bioorg. Med. Chem. Lett.* **2006**, *16*, 302–306.

(34) Carotti, A.; Stefanachi, A.; Ravina, E.; Sotelo, E.; Loza, M. I.; Cadavid, M. I.; Centeno, N. B.; Nicolotti, O. 8-Substituted-9-deazaxanthines as adenosine receptor ligands: design, synthesis and

structure–affinity relationships at A<sub>2B</sub>. *Eur. J. Med. Chem.* **2004**, *39*, 879–887.

(35) Papesch, V.; Dodson, R. M. Pyrimido[5,4-*d*][1,2,3]triazines. *J. Org. Chem.* **1963**, *28*, 1329–1331.

(36) Klotz, K. N.; Hessling, J.; Hegler, J.; Owman, C.; Kull, B.; Fredholm, B. B.; Lohse, M. J. Comparative pharmacology of human adenosine receptor subtypes—characterization of stably transfected receptors in CHO cells. *Naunyn-Schmiedeberg's Arch. Pharmacol.* **1998**, *357*, 1–9.

(37) Gessi, S.; Varani, K.; Merighi, S.; Cattabriga, E.; Pancaldi, C.; Szabadkai, Y.; Rizzuto, R.; Klotz, K. N.; Leung, E.; Mac Lennan, S.; Baraldi, P. G.; Borea, P. A. Expression, pharmacological profile, and functional coupling of A<sub>2B</sub> receptors in a recombinant system and in peripheral blood cells using a novel selective antagonist radioligand, [<sup>3</sup>H]MRE 2029-F20. *Mol. Pharmacol.* **2005**, *67*, 2137–2147.

(38) Borea, P. A.; Dalpiaz, A.; Varani, K.; Gessi, S.; Gilli, G. Binding thermodynamics at A<sub>1</sub> and A<sub>2A</sub> adenosine receptors. *Life Sci.* **1996**, *59*, 1373–1388.

(39) Borea, P. A.; Dalpiaz, A.; Varani, K.; Guerra, L.; Gilli, G. Binding thermodynamics of adenosine A<sub>2A</sub> receptor ligands. *Biochem. Pharmacol.* **1995**, *49*, 461–469.

(40) Varani, K.; Gessi, S.; Merighi, S.; Vincenzi, F.; Cattabriga, E.; Benini, A.; Klotz, K. N.; Baraldi, P. G.; Tabrizi, M. A.; Lennan, S. M.; Leung, E.; Borea, P. A. Pharmacological characterization of novel adenosine ligands in recombinant and native human A<sub>2B</sub> receptors. *Biochem. Pharmacol.* **2005**, *70*, 1601–1612.

(41) Varani, K.; Merighi, S.; Gessi, S.; Klotz, K. N.; Leung, E.; Baraldi, P. G.; Cacciari, B.; Romagnoli, R.; Spalluto, G.; Borea, P. A. [<sup>3</sup>H]MRE 3008F20: a novel antagonist radioligand for the pharmacological and biochemical characterization of human A<sub>3</sub> adenosine receptors. *Mol. Pharmacol.* **2000**, *57*, 968–975.

(42) Bradford, M. M. A rapid and sensitive method for the quantitation of microgram quantities of protein utilizing the principle of protein–dye binding. *Anal. Biochem.* **1976**, *72*, 248–254.

(43) Cheng, Y.; Prusoff, W. H. Relationship between the inhibition constant (*K<sub>i</sub>*) and the concentration of inhibitor which causes 50% inhibition (*I<sub>50</sub>*) of an enzymatic reaction. *Biochem. Pharmacol.* **1973**, *22*, 3099–3108.

(44) Munson, P. J.; Rodbard, D. Ligand: a versatile computerized approach for characterization of ligand-binding systems. *Anal. Biochem.* **1980**, *107*, 220–239.